Chemiresistive Nanosensors with Convex/Concave Structures

Songyue Chen,[a,*] Yongliang Tang,[a] Kan Zhan,[b,e] Daoheng Sun,[a] Xu Hou,[b,c,d,e,*]

[a] School of Aerospace Engineering, Xiamen University, Xiamen 361005, China, [b] State Key Laboratory of Physical Chemistry of Solid Surfaces, College of Chemistry and Chemical Engineering, Xiamen University, Xiamen 361005, China, [c] Research Institute for Soft Matter and Biomimetics, College of Physical Science and Technology, Xiamen University, Xiamen 361005, China, [d] Pen-Tung Sah institute of Micro- Nano Science and Technology, Xiamen University, Xiamen 361005, China, [e] Collaborative Innovation Center of Chemistry for Energy Materials, Xiamen University, Xiamen 361005, China.

Corresponding authors: s.chen@xmu.edu.cn (S. Chen), houx@xmu.edu.cn (X. Hou)

Abstract

Nanosensors have attracted tremendous, scientific and application, interests promoted by the advances in nanotechnology and emerging new nanomaterials. There has been rapid progress in developing chemiresistive nanosensors, and these sensor technologies are being transferred among a variety of different fields, from energy, environment to life science. This review presents nanomaterials with special convex/concave structures used for chemiresistive sensors, which mainly composed of one-dimensional conductive structures, e.g. nanowires, nanotubes, nanopores and nanochannels. Furthermore, designing, operation, and applications of current chemiresistive nanosensors are discussed to give an outlook of this field, especially for ionic solution and gas as the working chemical environments. The author hopes this review could inspire the active interest in the scientific field of sensor development and application.

Keywords

Nanosensor, Convex/Concave Structures, Nanowire, Nanopore/channel, Nanotube

1. Introduction

Since the emergence of nanosensors in the end of 1990s, their increasing applications have been ranging from chemical species detection [1-3] to label free sensing of biomolecules [4-8] and as medical indicators [9-11]. Resistive nanosensors, including nanowires (NW), nanotubes (NT), nanochannels/nanopores (NP) and their hybrid structures, possess a large surface-to-volume ratio, which renders them high sensitivity and new sensing mechanisms. Such one-dimensional nanostructures represent the minimum dimensionality for electric conduction and are applied in recording analyte adsorption or desorption process. They can be readily integrated into electronic devices for low cost and low power consumption devices, being amenable to miniaturization, scalability and electrical addressable multiplexed recording [12].

Resistance is generally measured by applying a voltage to the sensor and recording the current through it. When analytes interact with the sensing surface, e.g. gases, ions, nucleic acids, and proteins, resistance changes can be observed as a result of either enhanced or inhibited charge transfer inside nanodevices [13]. Three critical aspects involved in designing a chemiresistive nanosensor include nanostructure design, material design, and interface design. This review focuses on chemiresistive nanosensors that are convex, concave and heterogeneous curved structures, with nanowire, nanopore/nanochannel, and nanotube as representative structures respectively as shown in the top three cross-sectional images of Fig.1. The conductive materials vary for different configurations. Nanowires made of conductive materials can be used in either liquid or gas environment. Nanopores/nanochannels themselves are not conductive, therefore they need ionic solution to assist resistive sensing. Nanotubes as a heterogeneous structure possess both convex and concave structure, can be constructed as both nanowire and nanopore configurations. The curvature effects are enhanced with further reduced size. It has been demonstrated that the electrostatic screening is stronger in the vicinity of convex curved surfaces [14]. The bottom two figures of Fig.1 show the key examples of sensor configurations for electronic devices and ionic devices. We provide extensive review on each category, with the aims to promote potential application of chemiresistive nanosensors for gas, ionic, and biomolecule detection.

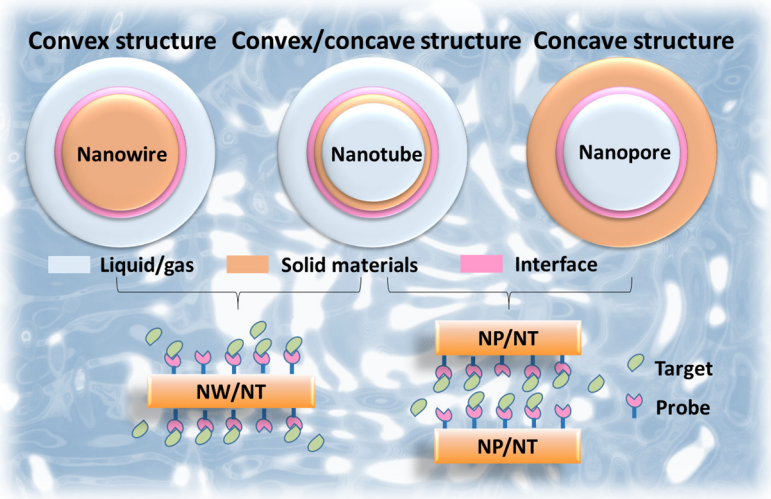

Figure 1 Transverse-section of nanosensors with different surface curvature structures: convex (nanowire, NW), convex/concave (nanotube, NT), and concave structures (Nanopore, NP) (top) and their main sensor configurations (bottom), with exterior wall as sensing surface for the left case and interior wall as sensing surface for the right case.

2. Convex structures

The typical representatives of convex nanostructure include nanowires, nanoparticles. Due to the limited dimension, nanoparticles have not been applied exclusively for resistive measurements, rather are used to form nanowires or a film so as to assist electron transfer [15]. Therefore, in this section, we will discuss convex structures in the form of NWs with five main conductive materials: metals, silicon, metal oxides, and conductive polymers.

2.1 Metal nanowires

2.1.1 Gas sensor

Metal NWs for gas sensing includes two working mechanisms, material modification (specifically Pd for hydrogen sensing), surface electron scattering (Au NWs [16] or Cu NWs [17] for molecular adsorption). The large amounts of electrons in metals limited the sensitivity of metal NWs and its applications.

The most popular metal for such application is Pd. Pd can adsorb hydrogen and form a bulk hybrid PdH*x*, which increase the electrical resistance of the material. Due to the large surface-to-volume ratio (SVR), palladium (Pd) NWs are expected to have short response and recovery times, and high sensitivity for gas sensing [18] or dissolved gas detection in a liquid [19]. Microfabricated Pd NWs showed a reversible detection of hydrogen concentration down to 27 ppm and response time of 5 s at concentrations over 20% [20]. Another less used sensing scheme for Pd NW sensing is based on morphological change of Pd metal structures at the presence of hydrogen [21]. The Pd grains expanse upon the adsorption of hydrogen, which closes nanogaps in between metal grains, and makes the nanowires conductive [22]. Such fractured NWs are applied at higher H_2 concentration, above ~2% dependent on the grain sizes [23]. Yang et al. [23] demonstrated that by increasing the Pd nanocrystalline grain diameter to 15 nm, the detection upper limit for the first sensing scheme can rise up to 10% without fracturing.

Pure Pd NWs undergo α- to β-phase transition at the loading and unloading of hydrogen, which causes embrittle of the materials [24]. Alloyed palladium, e.g. Pd-Au, Pd-Ni, is expected to suppress the phase transition, hence reduce the embrittlement and increase the operation time [24-26]. The sensor response behavior is dependent on the bimetallic composition [25]. In-situ fabricated Pd-Au alloy NW exhibited excellent hydrogen response with detection limit to be below 0.5% by volume [25]. Pd-Au alloys are shown to have improved adsorption to H_2.

Chemisorption of gas to noble metal NWs can also be measured by resistance change when the feature dimension is less than the mean free path of bulk metal electrons, in which case the resistance is dominated by surface scattering. Liu et al. [27] fabricated Au-Ag alloy NWs with feature size of ~ 10 nm for alkanethiol adsorption study. Adsorption of a monolayer of octadecane thiol results in 3% resistance change. A recent developed metal NW for gas sensing is Pt NW [28]. A Pt NW shows reversible resistance reduction for H_2 in air at concentration above 10 ppm. Pt based H_2 sensor can only be operated with the NW cross-sectional dimension near the mean free path of metal electron (~ 5 nm) [29]. The mechanism for the resistance decrease was explained by reduced electron scattering on Pt surfaces at the adsorption of H_2 compared with adsorption of O_2 [28, 30].

2.1.2 DNA sensor

Growth of metals on DNA template to form metal nanowires has been applied for DNA sensing [31-33]. The metal deposition process is facilitated by the selective precipitation of metal ions on the DNA through ion-exchange. Nobel metals such as silver [34], gold [32], copper [35], palladium [36, 37], and platinum [38] have been used for construction of metal NW electronic devices. Braun et. al. [34]confirmed for the first time the electron transfer inside such a DNA-templated silver NWs with 12 μm long and 100 nm wide. The fabrication process is shown in Fig. 2A. Two separate electrodes with 12 - 16 μm apart are firstly bridged by DNA hybridization to oligonucleotides that were previously immobilized to both electrodes through sulphur-gold interactions, followed by metallization of silver to the DNA skeleton. Electric current was observed at silver deposition on the bridge with a bias voltage applied. To adapt the idea for short DNA detection, Russell et. al. [32] designed a stretched rolling circle amplification (RCA) process that creates a long single-strand production on the electrode, as illustrated in Fig. 2B. Two electrodes with a gap of 5 μm was fabricated by photo lithography. To bridge the two electrodes, the RCA products is extended by the receding meniscus principle, which is realized by washing the RCA products with buffer and then drying the surface. The DNA is left attaching to both electrodes' surface. After DNA metallization with gold or silver, a very high signal-to-noise ratio readout can be obtained. Another idea raised by Weizmann et al. [33] was to form DNA-carbon NT hybrid structure connecting two electrodes. Conductance enhancement is observed after enzymatic silver metallization. A detection limit of 10 fM DNA analyte was achieved.

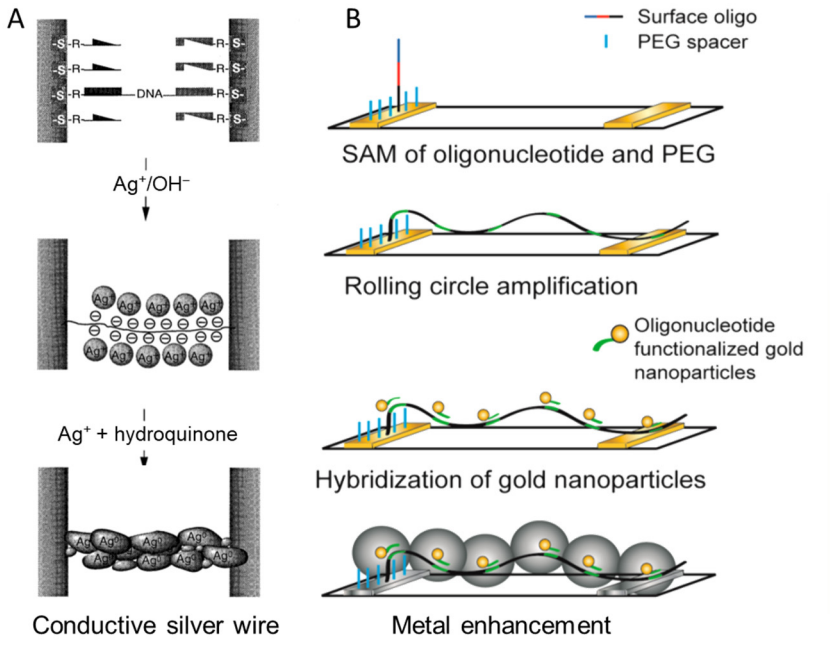

Figure 2 DNA-templated metal NW for sensing applications. (A) Silver NW formation on DNA in between two electrodes, by DNA hybridization to oligonucleotides on both electrodes, followed by metallization to the DNA skeleton with Ag^+ and metal enhancement. (Printed with permission from Reference [34]. ©1998 Nature Publishing Group.) (B) Metallization with gold nanoparticles for short DNA detection, by firstly forming a self-assembled monolayer (SAM) of oligonucleotide and poly(ethylene glycol) (PEG), proceeding the rolling circle amplification, followed by hybridization of gold nanoparticles and eventually metal enhancement. (Printed with permission from Reference [32]. ©2014 American Chemical Society.)

2.2 Silicon nanowires

Besides the increased SVR nanostructure brought, Si NWs are amenable to complementary metal-

oxide-semiconductor (CMOS) integrated circuits fabrication process, and therefore are recognized to be a next generation ultra-fast chemical sensing systems [39]. They have evoked substantial research activities on the applications as ionic sensors, biosensors, and gas sensors.

2.2.1 Ionic sensor

Ionic sensor or ion-sensitive sensor is based on transduction of ion activity in a solution into an electrical potential. A significant amount of work has been carried out on conventional ion sensitive field-effect sensors over the past 40 years [40-43] that can facilitate the full understanding and optimization of the sensing performance of NW sensors. Surface potential measurement is one of the most popular methods to transform target chemical or biological inputs into electrical signals. The interaction between the solvent or solute molecules and the sensor surface modifies the nanometer-scale double layer capacitance in the vicinity of the interface [44]. The resultant surface potential change causes enhanced electrical signal for nanosensor, which can be measured by the threshold voltage shift of NW field-effect transistor (FET) devices [45, 46], conductance change [1, 47, 48], frequency spectrum [49] or ion-step method [50]. An inorganic dielectric material, such as SiO_2 [1], Al_2O_3 [47], and HfO_2 [51], are formed as the gate-oxide, which interfacing between the device and solution. The oxide surface exposed in solution can be described by the site-binding model when only hydroxyl group is reacting with the electrolyte [43], which describes the relationship between the bulk pH, oxide surface charge density and surface potential. Ionic sensing is realized when a pH change or ion addition induced surface potential change causes a measurable conductance change through a field-effect across the dielectric oxide layer. The fact that surface potential change is dependent on certain ionic concentration of the electrolyte forms the basis of the ion sensitive FET [40-42] sensors.

The pH sensing study on Si-NW devices was initially done to characterize NW device properties [1, 52]. The gate oxide undergoes both protonation and deprotonation when exposed to electrolyte, as illustrated in Fig. 3A. A bare SiO_2 gate surface shows a non-linear response for pH measurements from 2 to 10, especially at low pHs [1]. Surface modification to SiO_2 with 3-aminopropyltrethoxysilane brings $–NH_2$ to the surface. The protonated $–NH_3^+$ from $–NH_2$ group at low pH act as a positive gate, which depletes the hole carriers in p-type NW and reduces the conductivity. The non-passivated –SiOH is deprotonated to $–SiO^–$ at high pH, and act as negative gate for hole accumulation. The combined acid and base behavior results in a linear response between the conductance change and pH values of the electrolyte [1]. The pH sensitivity can be further improved by atomic layer deposition of alumina (Al_2O_3), which offers more active surface sites and obtains near Nernstian response (57.8 mV/pH) [47].

Besides protons, alkali ion can be sensed, especially after surface chemical modification. Chen et al. [50] reported that the current through Si NWs was responsive to the potassium ion concentrations induced surface potential change. Metal ions induced cross reactivity on oxide surface is however not selective to oxide surface. Therefore, Cui et al. [1] functionalized calmodulin onto Si NW surfaces to achieve selective sensing of Ca^{2+} ion. Luo et al. [53] reported selective Hg^{2+} and Cd^{2+} ions detection at a detection limit of 0.1 μM and 0.1 mM with a 3-mercaptopropyltriethoxysilane modified Si NWs. Wipf et al. [54] designed sodium ion sensor by self-assembled monolayer of thiol-modified Na^+-selective crown ethers on a gold layer that was deposited beforehand on silicon nanowires (Fig. 3B). To eliminate the influence of other ions, e.g. Cl^-, H^+, K^+, differential measurement scheme was designed with a response sensitivity of 44 mV/dec (Fig.3B(right)).

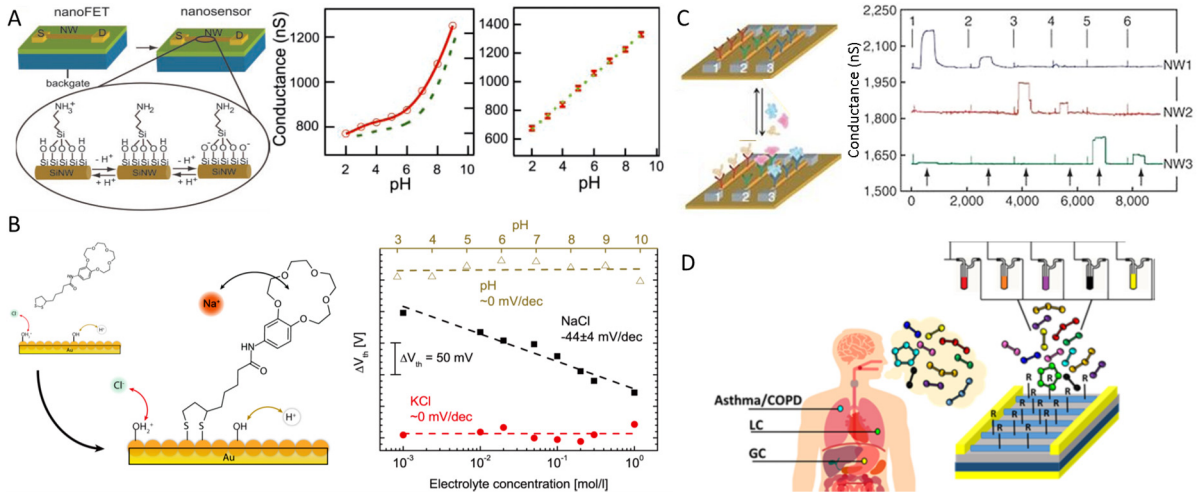

Figure 3 Si NW-based chemiresistive sensors. (A) pH sensing comparison between SiO_2 surface with non-linear response (middle) and amine functionalized surface with linear response (right). (Printed with permission from Reference [1]. ©2001 American Association for the Advancement of Science.) (B) Sodium ion sensing with sodium selective crown ethers immobilized: surface functionalization scheme (left) and threshold voltage change measurement on different ions (Na^+, K^+, H^+) with differential setup (right). (Printed with permission from Reference [54]. ©2013 American Chemical Society.) (C) Multiplexed protein biosensing for cancer markers monitoring. (Printed with permission from Reference [55]. ©2005 Nature Publishing Group.) (D) VOC gas sensing in complexed gas compounds with a multiplexed sensing scheme. (Printed with permission from Reference [56]. ©2015 American Chemical Society.)

2.2.2 Biosensor

There has been a large variety of applications featuring NW sensors since their first introduction as biosensors in 2001 [1]. Binding of charged biomolecules can both affect the vicinity of the surrounding environment, e.g. ionic distribution, electrical field, and change the material electrical properties [57]. Si-NWs have been demonstrated for highly sensitive detection of surface potential changes induced by the association or dissociation of various biological analysts, such as proteins[1, 12, 48, 55, 58-60], nucleic acids [61-65], viruses [66], tissues [67] and cellular bioelectricity/biochemistry [68-71] from NW surfaces [9, 10, 72, 73]. Probe molecules can be immobilized on NW surface covalently, e.g. by silane chemistry [1, 48], electrostatic adsorption [74, 75] or Si-C chemistry [62, 76]. Immobilization of charged target biomolecules on NW surface induce surface potential changes and can thus gate NWs. Figure 3C shows a multiplexed protein detection of cancer markers with NW array, enables discrimination against false positives. The detection limit for DNA in low ionic solution has reached fM level [61, 65], while for cardiac troponin I is as low as 0.092 ng/ml [77]. To improve the sensitivity, uncharged probes, e.g. peptide nucleic acid (PNA) as a replacement to DNA or RNA probes [61, 63, 64], are introduced especially for detection in low ionic strength solutions. PNA hybrids have higher thermal stability and work even at low ionic strengths.

Since the NW sensors detect a surface charge density change, so it is critical to consider the screening of ions to the target biomolecules. The Debye length is a measure of the distance that the dissolved ions extend away from the surface. We generally need Debye length to be larger than the total length of the ligands so as to prevent charge screening [78-81], as illustrated in Fig. 4A. Although detection in low ionic solution (< ~1mM) is the most commonly used method to guarantee required Debye length, the real-life application generally includes much higher ionic strengths.

Detection in biological fluidics has been a leading potential approach for sensors to clinical use [59], e.g. for the early detection of precancerous lesions from biological fluidics [82], or a cancer prognostic protein marker in serum [83]. Aiming for such applications, Gao et al. [84] designed a general strategy by incorporating a biomolecule permeable polymer layer on the sensor to extend the effective screening length, as shown in Fig. 4B. Prostate specific antigen can be detected with a sensitivity of 10 nM in 100 mM PBS. Elnathan et. al. [85] proposed a biorecognition layer engineering method to overcome the screening limitations. They constructed size-reduced antibody fragments that permits the adsorption events occur in closer vicinity to the NW surface, as illustrated in Fig. 4C. Biosamples such as serum and untreated blood, are highly complex solutions, result in a significant background noise for analytical measurement. Detection of antigens in complex untreated biosamples with Si NWs by application of antigen-dissociation regime, which can overcome the Debye screening limitation of NW-based biosensors [86]. Fast wash-out of the device with low ionic-strength buffer reveals two distinct separable dissociation regimes. A slower dissociation rate of the target antigen from Si NW can be observed. Besides, surface probing molecule alignment by electrical field is proposed [87] for improving NW sensitivity (Fig. 4D). A well-aligned monolayer can greatly enhance collective charge polarization brought by molecular interaction. They argued that the alignment process works both for polar and nonpolar molecules, with sensitivity improvement by up to 3 orders statistically.

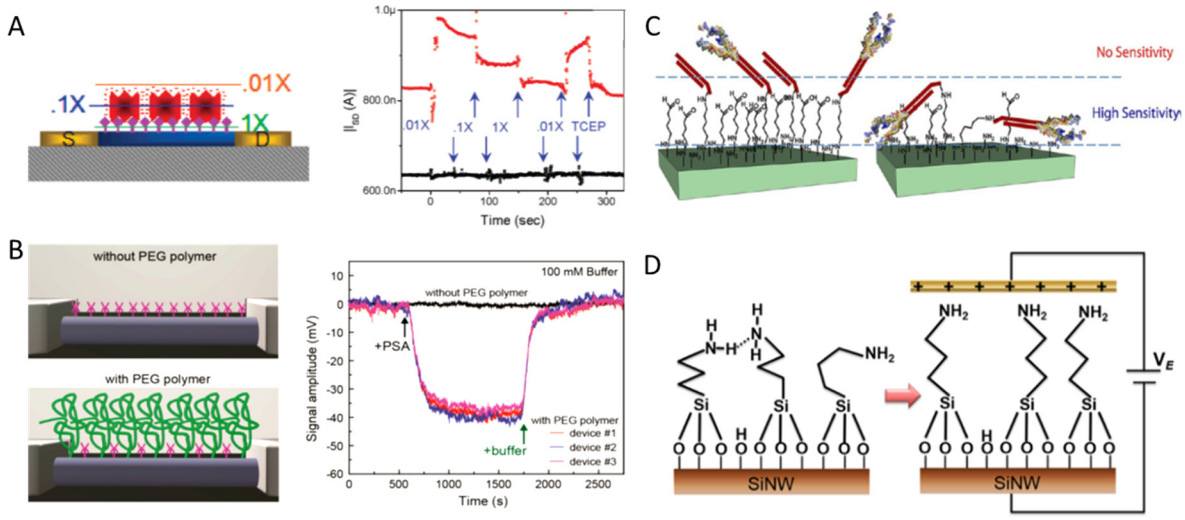

Figure 4 Interface engineering for sensitivity improvement by (A) Debye length control with ionic concentrations, (B) PEG polymer surface modification to increase the screening length, (C) probe layer engineering to bring probe closer to the sensing surface, and (D) probe alignment with electric field. (Printed with permission from References [81], [84], [85], and [87]. ©2007, 2015, 2012, 2013 American Chemical Society.)

To further improve the sensitivity, specific attachment of probe molecules to NWs are developed. One disadvantage of Si NW sensor with SiO_2 interface is the homogeneously distributed oxide surface on the entire substrate surface. Therefore, Li et al. [88] treated the Si NWs with an amino silane gas before transferring to a substrate, resulting in increased sensitivity with single protein detection capability. This method works only for bottom-up fabricated NWs that requires wire transfer. For top-down fabricated NWs, one strategy is to apply Si-C chemistry to Si NWs. Si NWs without native oxide exhibit not only improved gating effect, and also enhanced selective functionalization [62, 76]. Si-C monolayer can be formed on Si surface directly with heterogeneous alkyl and alkenyl groups that can further attach biomolecular moieties. Bunimovich et al. [62] constructed such an interface for DNA detection

in physiological electrolyte with 0.165 M ionic strength. By removing the native oxide, the sensor exhibits 2 orders of magnitude improvement in the sensing dynamic range.

2.2.3 Gas sensor

Si NWs are reported to be sensitive to a variety of gas molecules, such as ethanol, hexane, toluene[89-91], and O_2, NH_3, NO_2 [92-94]. The variation of dipole moment and/or electrostatic effect for polar molecules induces electrical current variation in Si NWs. The sensing mechanism for nonpolar molecules is based on the indirect interaction between the analytes with the modified molecules on the NW surface through molecular gating, while the dielectric constant, the effective dipole moment of the organic layer, and/or the interface state density are affected [89, 95]. Oriented at real-world clinical usage, Shehada et al. [56, 96] developed Si NW gas sensor for noninvasive detection of volatile organic compounds (VOCs) linked with various disease breath prints. The working scenario is illustrated in Fig. 3D. Exhaled breath is one of the most convenient VOC sources for monitoring the state of health noninvasively. A list of VOCs is detected selectively by lock-and-key approach to adapt the cross-reactive sensor arrays for complex breath samples. Individual surface modification to each NW by silane chemistry is performed to passivate the surface states and to optimize the interaction of VOCs with the NW surface, e.g. trichloro(phenethyl)silane for cancer VOCs detection [56]. To analyze the complex gas compounds, multiplexed sensing scheme is designed for independent sensing of individual compounds. After initial feature selection, artificial neural network analysis was used for disease diagnosis, with $>$ 80% accuracy.

The density of non-passivated Si-OH groups act as trap-states on the surface, and thus play a vital effect on the hysteresis characteristics of the sensors [97]. Trap-states reduction realized by removing the NW oxide layer and functionalizing the surface with non-oxide C3 alkyl groups, higher sensor stability and accuracy were obtained by Haick's group[90]. The most stable and sensitive sensor for nonpolar analytes is the propenyl -modified sensor, compared with propyl and propynyl modifications. However, each surface type has its pros and cons when investigating sensor properties comprehensively, e.g. gas type/polarity identification capability, sensitivity, selectivity and stability. Therefore, a combination of these sensors is suggested for obtaining the best performance.

Another important application of Si NW gas sensor is for explosive chemical detection. Engel et al. [98] constructed APTES monolayer modified Si NWs for 2,4,6-trinitrotoluene (TNT) explosives detection at concentration as low as 1 ppb. TNT molecules bind strongly to the NW surface through an acid-base pairing interaction between TNT and amino groups. The binding of electron-deficient TNT to the amino ligands leads to the formation of charge-transfer complexes. The sensor can specifically distinguish TNT form other related compounds and allows for detection directly from samples in air.

2.3 Metal-oxide nanowires

Metal-oxide NWs are typically used for gas sensing, although a few demonstrations can be found for biosensor usage, e.g. TiO_2 NWs for IgG detection through electrochemical coating of a low-conductivity polymer layer [99].

2.3.1 Gas sensor

N-type metal oxide semiconductors, e.g. ZnO, In_2O_3, SnO_2, based on which chemical nanosensors are

studies [100], have conduction electrons primarily originated from point defects. The adsorption and desorption of gas molecules on the structure surface modifies the carrier concentration, resulting in a change of resistance [2, 101]. The resistance may increase or decrease at gas adsorption, which depends on the dominant charge carrier in NWs and type of gas interacting with the surface. It has been demonstrated that metal oxide-based NW sensor are capable of detecting both reducing and oxidizing gases, such as H_2, CO, ethanol and O_2, Cl_2, CO_2. Take Cl_2 as example, the sensing mechanism is based on Cl_2 adsorption on the oxide surface and oxygen vacancy and formation of Cl^- at low temperature (below 200°C), which increase the resistance of the nanowire. However, the mechanism changes when measured at higher temperature (300°C). The substitution of chlorine molecules for pre-adsorbed oxygen and lattice oxygen result in decrease of resistance [102, 103]. SnO_2 nanowires exhibits higher sensitivity to Cl_2 gas than ZnO and WO_3 nanowires, at the ppb level, and ZnO nanowire sensor can be applied for high Cl_2 concentration monitoring at the ppm level [103]. It's possible to control ZnO nanowire orientation and defects to modulate the gas sensing properties [104]. The high sensitivity and reversibility of such sensors under ambient conditions is attributed to the intrinsically small grain size and high SVR of the NW [105].

A few methods have been studies to improve the sensing performance, including elevated operation temperature and surface decoration. One unique advantage of resistive sensors is their self-heating effect. For gas sensing, operation of metal oxide sensor at elevated temperature accelerates molecule desorption and recovery of sensor surface [106, 107]. Prades et al. [108] presented self-heated individual SnO_2 NWs towards NO_2 sensing, and proved that the performance is comparable with conventional integrated microheaters. Surface decoration with noble metal nanoparticles to metal oxide NWs enhances gas sensitivity [109]. Kolmakov et al. [110] observed increased catalytic dissociation of the molecular adsorbate on the surfaces after Pd particle functionalization to SnO_2 NWs. Zou et al. [111] decorated Mg-doped In_2O_3 NWs with metal nanoparticles (i.e. Au, Ag, and Pt), and obtained more than three orders of magnitude response increase to 100 ppm CO, with ~4s corresponding response time and detection limit of 500 ppb.

2.4 Conductive polymer nanowires

Conductive polymeric (CP) NWs including polypyrrole (PPy), polyaniline (PANI), poly(3,4-ethylenedioxythiophene) (PEDOT) and polythiophene (PT) have been used as an alternative material to metal and semiconducting NWs for chemiresistive sensing. Conductive polymer NWs offers many advantages compared with inorganic materials, e.g. low cost, easy fabrication, tunable conductivity, high porosity and high flexibility [112-114]. For example, the conductivity of PANI can be modified by non-redox acid doping/base dedoping process [115].

2.4.1 Gas sensor

Polar molecules can either dope or dedoped conductive polymers, in other words, oxidize or reduce the state of polymer materials, which resulting in a decrease or increase in resistance depends on the type of carriers in the polymer material. P-type conducting polymer shows loss in charge carriers number due to dedoping upon ammonia adsorption. The reversible reaction with adsorption and desorption renders sensing and recovering of the sensor accomplished simply by changing the exposing gas. Gas adsorption induced inherent oxidation state change can be observed with PANI conductivity change [112]. Conductometric gas sensor based on PANI NWs were investigated for H_2

detection as low as 0.5% and CO detection at 1ppm [116]. Wang et al. [117] reported PPy and PEDOT NWs with highly oriented crystalline structures for real-time detection of ammonia gas and ethanol vapor in parallel. Both NWs response sensitively and quickly at the presence of saturated ethanol vapor. However, PEDOT NW showed little change upon exposure to ammonia gas compared with PPy NWs, and is regarded as selective sensor towards ethanol. To get more sensitive and faster response, smaller diameter of wires are suggested to speed up gas molecule diffusion in NWs [118]. A well-defined PEDOT:poly(styrenesulfonate) NWs of sub-100 nm by nanoscale soft lithography showed a fast detection limit of ppb level for NH_3 and NO_2 gas [119].

Besides single gas composition detection, polymeric NWs have also been demonstrated as electronic nose for gas mixture classification. Song et al. [120] constructed PANI NW sensor array for multi-analyte detection. Each sensor responds differently and results in a unique fingerprint for each mixture, therefore, chemical species can be differentiated by a pattern recognition algorithm.

2.4.2 Biosensor

CP for biomolecule sensing have been demonstrated on bulk materials [121]. Biomolecule probes, e.g. proteins [122, 123], oligonucleotides [124], glucose [125, 126], have been incorporated in the polymer NW by attaching to a monomer before polymerization, entrapment during synthesis, or conjugation after synthesis. The sensing mechanism is based on the conductance change with the attachment of target molecules, as shown in Fig. 5A. Ramanathan et al. [123] fabricated single and multiple individually addressable PPy NWs, which was functionalized with avidin by electropolymerization when pyrrole monomer and dopant is defined in a single step. The NW resistance increase rapidly upon addition of 1 nM biotin-conjugated DNA solution. Bangar et al. [127] established covalent surface functionalization chemistry of antibody with glutaraldehyde and N-(3-dimethylaminopropyl)-N-ethylcarbodiimide hydrochloride for cancer antigen CA 125 detection with PPy NWs. The fabricated PPy NW is shown in Fig. 5B. The sensor showed a detection limit of 1 U/mL CA 125 in 10 mM phosphate buffer. Later the same research group [124] functionalized ssDNA on single PPy NW using a linker molecule and thiol chemistry for breast cancer gene detection. A detection limit of sub-fM is achieved in 10 mM buffer solution after carefully tuning the DNA base length and monitor the work function change of the NWs. Bigger biomolecules such as viruses have also been incorporated into PEDOT NWs for sensing various proteins as studies by Arter et al. [122, 128], with the measurement setup illustrated in Fig.5C. By electropolymerizing M13 bacteriophage into PEDOT NWs, a prostate cancer marker can be detected. Resistance change is monitored with prostate-specific membrane antigen concentration from 20 to 120 nM in high ionic strength buffer [128]. Despite the advantage that conductive polymer NWs brought, there are still challenges remaining for commercial application, such as environmental stability, multiplexed detection, miniaturization and integration.

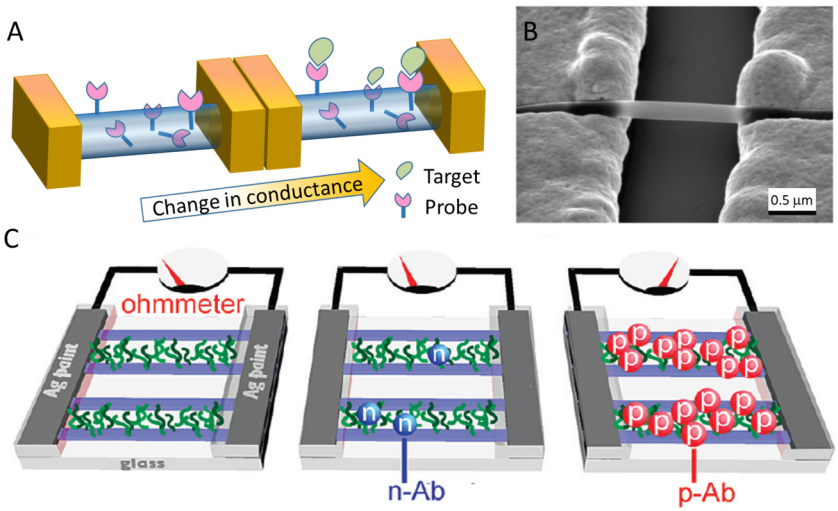

Figure 5 Polymer NW based chemiresistive sensor. (A) Schematic of polymer NW with probe embedded for biosensing applications. (B) scanning electron microscopy image of a PPy NW sensor for antigen detection. (Printed with permission from Reference [127]. ©2009 American Chemical Society.) (C)Virus-poly(3,4-ethylenedioxythiophene) (PEDOT) NW device for resistance-based measurement: no resistance change with negative control antibody (n-Ab) and substantial resistance change with positive antibody (p-Ab). (Printed with permission from Reference [122]. ©2010 American Chemical Society.)

3. Concave structures

Typical concave nanostructures for resistive sensing includes nanopores and nanochannels. In this section, we will discuss the typical constructions, working mechanisms and applications of such sensors, with focus on protein nanopores, polymer nanopores and inorganic nanopores and nanochannels. Structure of protein nanopore is mainly related to a typical protein (α-haemolysin, αHL). The working mechanism for nanopore/nanochannel resistive sensor includes resistive pulse recording of molecule transport through a NP/NC (Fig. 6A), e.g. DNA sequencing, steady-state conductance change measurement at the ambient stimuli (Fig. 6B) or target biomolecule (Fig. 6C) immobilization on the inner walls of the NP decorated with recognition sites [7]. The first scheme is mainly based on the volume exclusion effect, while the second scheme is mainly an electrostatic effect [129]. The related applications of nanopores include ionic sensing, biosensing, and gas sensing.

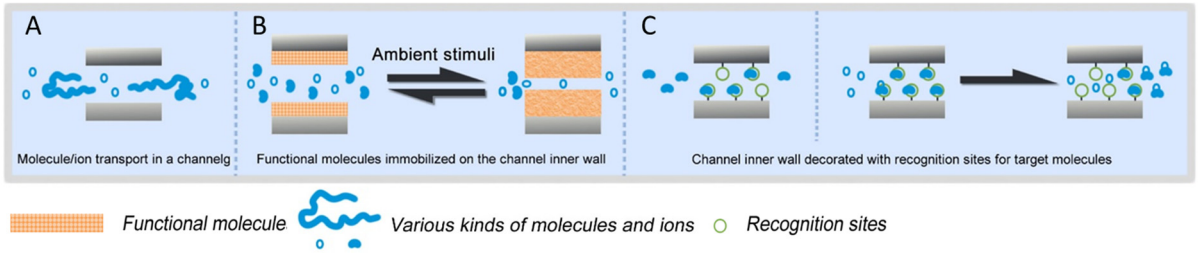

Figure 6 Construction of chemiresistive sensors based on nanopores. (A) Sensing based on molecule/ion transportation. (B) sensing of various molecules and ions as ambient stimuli in nanopores. (C) sensing by capturing or releasing of target molecules from the recognition site inside nanopores. (Printed with permission from Reference [7]. ©2009 American Chemical Society.)

3.1 Protein nanopores

Protein nanopores are present in cell membranes [130] for controlling ions and molecule transport

through the membranes [131, 132]. For example, αHL protein nanopores (Fig.8A) are assembled by αHL monomers with a known heptameric pore structure [133]. The αHL protein nanopores have the benefit in sensing application from metal ions, small molecules, reactive molecules, DNA and proteins because of their high resolution and stability [134, 135]. The recording signal represented by ionic current features the translocation process. Figure 8D shows the single-channel recordings comparing permanent and transient adapter [136].

3.1.1 Ionic sensor

The transport of ions through the cell membranes is a basic feature in life processes. Transportation often includes very precise selectivity for specific ions [134]. Fig. 7C illustrates four different architectures of ion channel and ion pump proteins in cell membranes. Inspired from the natural membranes, protein nanopores are excellent prospects as components of biosensors to detect simple ions [137-140]. Braha et al. [138] investigated that a single sensor can detect several metal ions including Zn^{2+}, Co^{2+}, Cd^{2+}. Furthermore, two metal ions can be analyzed simultaneously, which imply the protein sensor can be a good candidate for detecting metals. Bayley et al. [139] fabricated the αHL protein nanopores with a heteromeric form to detect the divalent ions. Wen et al. [141] detected Hg^{2+} selectively by forming duplex with properly designed ssDNA, which changed the translocation property of the ssDNA through αHL nanopore (Fig. 7D). To achieve sensitive and selective detection of cupric ions, polyhistidine molecule as a chelating agent is added to the solution that as well altered the translocation profile [142].

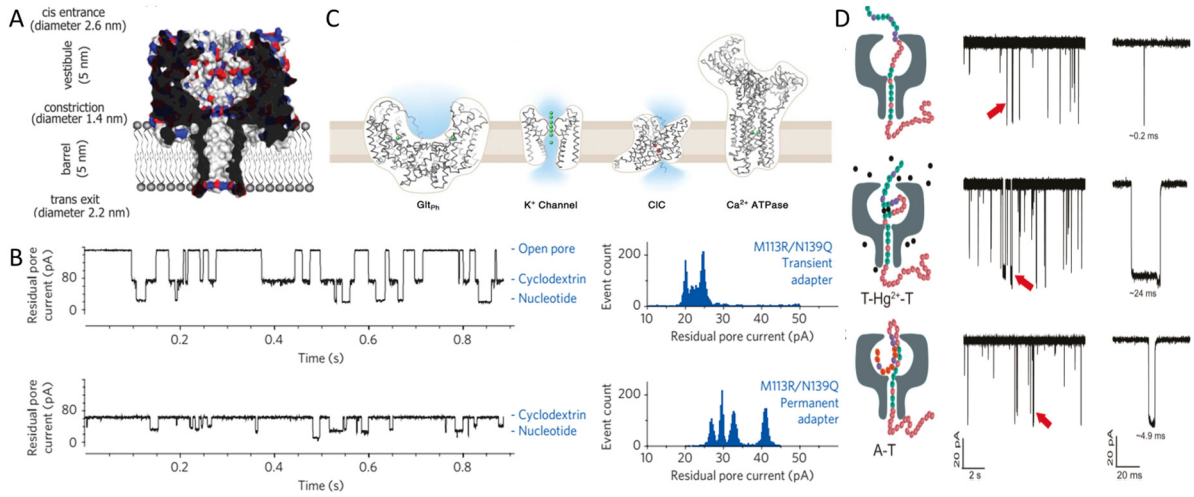

Figure 7 Protein nanopore sensor for resistive-pulse measurements. (A) Section through the αHL nanopore. Charge distribution in the αHL nanopore, amino acids with positive and negative charge are blue and red color, respectively. (Printed with permission from Reference [134]. ©2008 The National Academy of Sciences of the USA.) (B) Single-channel recordings comparing permanent and transient adapter: αHL pore with transient adapter binding show nucleotide detection (up). αHL pore with permanent adapter show continuous nucleotide detection (down). (Printed with permission from Reference [136]. ©2009 Nature Publishing Group.) (C) Architectures of ion channel and ion pump protein in cell membranes: sodium-dependent glutamate transport pump, a model of K^+ channel, funnel-shaped structures are located in chloride channel (ClC) proteins, and a structure of the calcium-bound form of the Ca^{2+} ATPase. (Printed with permission from Reference [130]. ©2005 American Association for the Advancement of Science.) (D) Translocation of ssDNA, DNA-Hg^{2+} hairpin and natural DNA hairpin through a single αHL nanopore. (Printed with permission from Reference [141]. ©2011 American Chemical Society.)

3.1.2 Biosensor

Protein nanopore DNA sequencing provide an effective way that can be performed without the need for labelling and complicated procedures.[136, 143]. Increased growing in the costs and demand of DNA sequencing has a great effect on genome research because understanding the genetic disease contributes to the developments of diagnostics and treatments [136]. In 2006, Bayley et al. [143] reported single DNA sequencing method to identify ribonucleotide and 2'-deoxyribonucleoside-5'-monophosphates by utilizing a protein nanopore equipped with a molecular adapter. Furthermore, such a method also achieves stochastic sensing by inserting a nanometer sized pore in an insulating lipid bilayer membrane. However, compared to the favorable approach, this method need to overcome the drawbacks that improving the accuracy of the nucleic acid base identification. They later reported a covalently attached adapter molecule for protein-nanopore, which can continuously identify unlabeled nucleoside 5'-monophosate molecules with accuracies of 99.8%, suggesting that protein nanopore is a highly accurate tool and suitable for sequencing nucleic acid [136].

3.2 Polymer nanopores

Inspired from the ion channel of the natural cell membranes [144, 145], scientists start to investigate the ionic sensing and biosensing by a synthetic polymer-based nanopore and nanochannel [146-155]. Compared with the biological protein nanopores, polymer nanopores offer many characteristics such as flexible preparation, easy modification, large-scale fabrication, shape and size controllability, and tunable surface charge properties [149, 151, 156]. In this section, we focus on the characteristics, typical constructions, and applications of polymer nanopore-based sensors. Commonly used polymer membranes for nanopore fabrication include poly(ethylene terephthalate) (PET), polyimide (PI), polycarbonate (PC) etc. [157, 158] Track-etching is a typical fabrication method to obtain the nanopores on the basis of polymer materials [157, 159-163]. This method utilize the energetic heavy ions to irradiate the dielectric film, followed by the chemically etching to obtain pores with desired dimensions [164]. This method provides both symmetric and asymmetric nanopore for a variety of applications such as ionic sensing and biosensing.

3.2.1 Ionic sensing

Ion channels, which regulate ion permeation through cell membranes, are especially important for the physiological functions in life processes. Therefore, it is significant to simulate these processes by a convenient artificial system [165]. Xia et al. [166] demonstrated a pH sensitive nanochannel with DNA molecule motor attached to the inner wall. As illustrated in Fig. 8A, at high pH, the DNA molecule relaxes to a loosely packed form that increase ionic current through the channel. Hou et al. [167] developed potassium responsive nanopore device based on G-quadruplex DNA functionalized nanopore surface to investigate the application of alkali ion sensing (Fig. 8B). In this system, the conformational change of G-quadruplex DNA is monitored by current change with Li^+ as control. A remarkable difference between K^+ ions and Li^+ ions can be observed over a concentration range of 0 to 1500 μM. To achieve selective potassium ion recognition, Perez-Mitta et al. [168] immobilized crown compounds 18-crown-6 units on a single asymmetric nanopore walls, as shown in Fig. 8C. Nanopore surface charge can be modified in the presence of alkali ions. The current rectification effect is obvious when replacing 0.1 M NaCl with 0.1 M KCl. The transmembrane ion current can be tuned over a large range of K^+ concentrations, which can be a potential nanofluidic devices for ionic sensors. Besides aforementioned homogeneous nanopore structures, there has been a rapid progress in developing

multi-scale heterogeneous nanochannels with symmetric/asymmetric modification for bio-inspired ion channel construction and applications[129, 156, 169, 170].

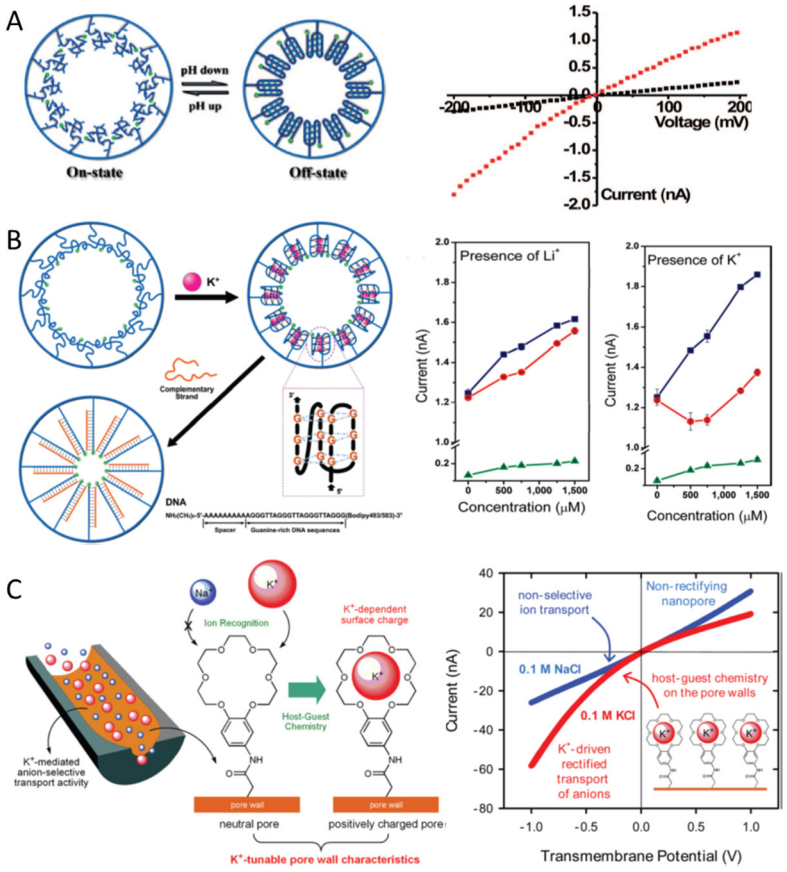

Figure 8 Ionic sensing with polymer nanopores. (A) pH sensing with DNA molecule motor immobilized on the inner wall. Increased current is observed from the IV curve by increasing pH4.5 (black) to pH8.5 (red). (Printed with permission from Reference [166]. ©2008 American Chemical Society.) (B) K^+ ionic sensing as modified by G4 DNA molecules (left), and current measurements for different Li^+ and K^+ concentration: before DNA modification (blue), after DNA modification (red) and after the addition of the complementary DNA strands (green) (right). (Printed with permission from Reference [167]. ©2009 American Chemical Society.) (C) Selective potassium sensing with crown compounds as recognition site (left). IV curve shows the difference in ion-current rectification degree for non-functionalized nanopore and functionalized nanopore (right). (Printed with permission from Reference [168]. ©2015 Royal Society of Chemistry.)

3.2.2 Biosensor

Biosensing performance with polymer nanopores depends on the surface charge of the materials and chemical groups decorated on the inner wall for specific binding of analytes [158, 171-173]. The analyte binding and molecule size can be detected as a change of the ion-current by monitoring the current blockage time [174, 175] or the ion-current rectification degree[176]. By electrostatically attaching biorecognition sites on the inner wall, Ali et al. [177] realized selective protein detection as illustrated in Fig. 9A. The positive charged $-NH_3^+$ anchoring agent form stable ligand layer to the negatively charged wall. To minimize the pore surface charge and improve the charge sensitivity to the target DNA, they [178] immobilized uncharged PNA probes on the surface through carbodiimide coupling chemistry (Fig. 9B). Single conical nanopores are fabricated in polyimide membrane for the sequence specific detection of ssDNA oligonucleotides. The surface charge density of the pore surface increase upon the PNA/DNA hybridization, as confirmed by IV curve changes. Such a method provides

a platform for the detection and discrimination of the short single-stranded DNA sequence. Mara et al. [171] investigated a DNA sensor based on a single nanopore fabricated in a PI membrane by a single heavy ion track-etching technique. The nanopore is 12 µm long that contributes a higher temporal resolution for DNA detection. Polymer nanopores also can be utilized to sense large DNA. Harrell et al. [179] describe resistive-pulse (or stochastic sensing method) sensing DNA based on a conical shaped nanopore in a PC membrane. This nanopore has a tip opening diameter of 40 nm and a base opening diameter of 1.5 µm. The frequency of DNA translocation events increase linearly with DNA concentration and the applied electric field. By integrating a more complex DNA structure inside the nanopores, Liu et al. [180] obtained significant signal amplification, with schematic shown in Fig. 9C. Channel interface modification by depositing a thin metal layer provides alternative surface chemistry for molecule immobilization [3, 174]. Therefore, a nanopore system based on polymer matrix allows a versatile surface modification that control the interface properties, which serves a blueprint to design biosensors.

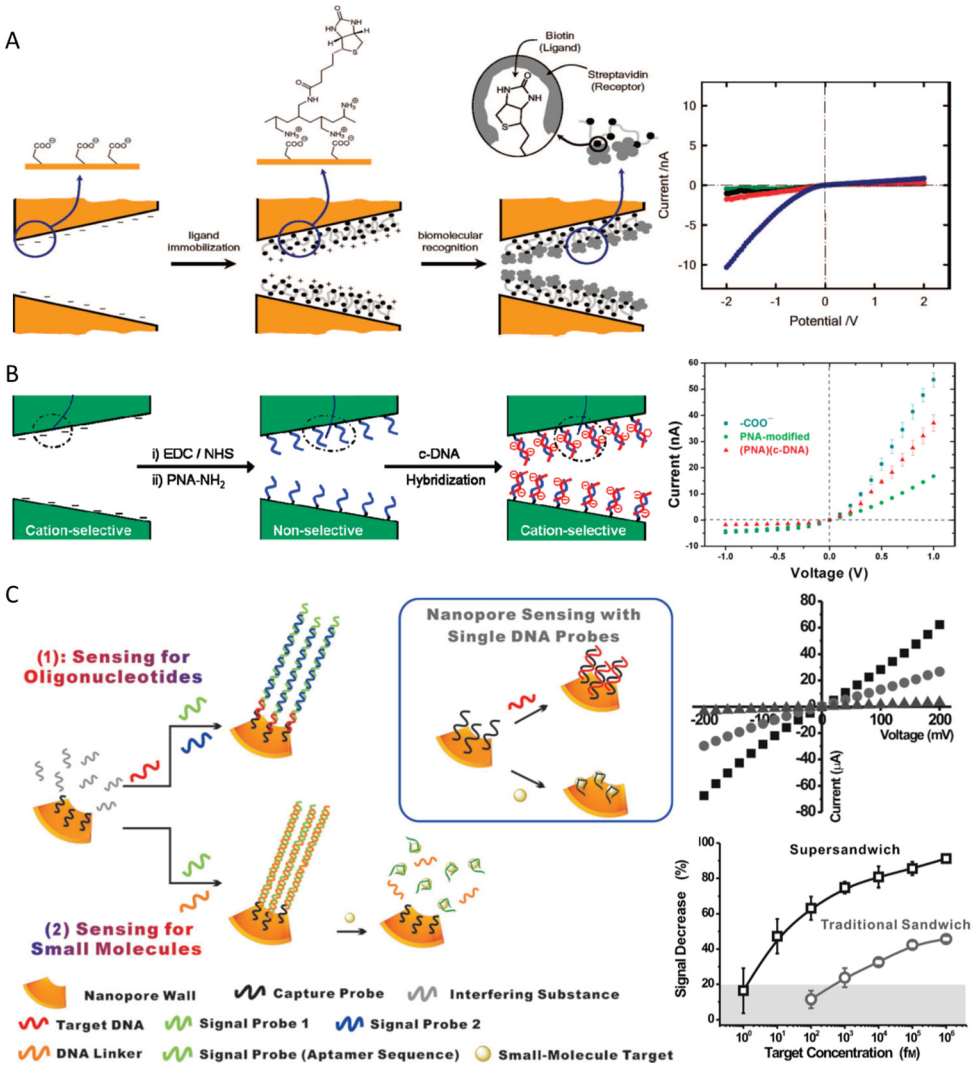

Figure 9 Polymer nanochannels used for biosensing. (A) Protein sensing scheme based on biotin modified inner wall for streptavidin detection (left), with IV curve shows the ion-current rectification degree change after streptavidin attachment (right). (Printed with permission from Reference [166, 177]. ©2008 American Chemical Society.) (B) DNA sensing based on PNA immobilized inner wall to minimize the surface charge (left) and the IV curve after each process (right). (Printed with permission from Reference [178]. ©2010 American Chemical

Society.) (C) Integrated DNA supersandwich structures for specific sequenced oligonucleotides and small molecules sensing (left): the IV curve before and after treatment with 10 fM and 1 nM target DNA (right up), and obvious signal amplification compared with traditional sandwich structure (right bottom). (Printed with permission from Reference [181]. ©2015 Wiley-VCH.)

3.2.3 Gas sensor

Nanopores for gas sensing, which is inspired by the odorant-gated ion channels in animal's olfactory sensory neurons (OSNs), is based on gas solubility in solution [182, 183]. The key element for such sensors is to construct gas reactive sensing material on the inner wall of nanopores. Xu et al. [182] grafted an imidazole-containing monomer to PET nanopore surface by atom transfer radical polymerization method. Imidazole undergoes protonation and deprotonation when the pH varies, is a suitable molecule for CO_2 sensing. The CO_2 concentration in the solution modulates the surface charge and wettability, and is measured by the ionic current change in the nanopore. Bubbling of CO_2 into the solution opens the pore and the ionic current increased 100 times. To improve the sensitivity and selectivity, Shang et al. [183] immobilized CO_2-responsive molecules APTE (1-(4-amino-phenyl)-2,2,2-trifluoro-ethanone) on the polyimide nanopore surface, and obtained an ionic current increase of 800 times after bubbling CO_2. Selectivity to CO_2 against 7 different gases is verified.

3.3 Inorganic nanopores

3.3.1 Ionic sensor

Glass nanopores functionalized with a macrocyclic dioxotetraamine derivative (C5) enable sensitive detection of Hg^{2+} ions [184]. The formation of Hg^{2+} and C5 complex on the inner walls converts the glass nanopore from a rectifying state to a non-rectifying state (Fig. 10A). The ion current rectification ratio differences demonstrate detectable Hg^{2+} concentration range from 10 pM to 1 mM. Single glass nanopore for selective detection of Cu^{2+} ions is reported by employing a cupric selective chelating agent, polyglutamic acid, as illustrated in Fig. 10B [185]. The formation of chelated Cu^{2+} ions on the nanopore induced a significant decrease of ion current.

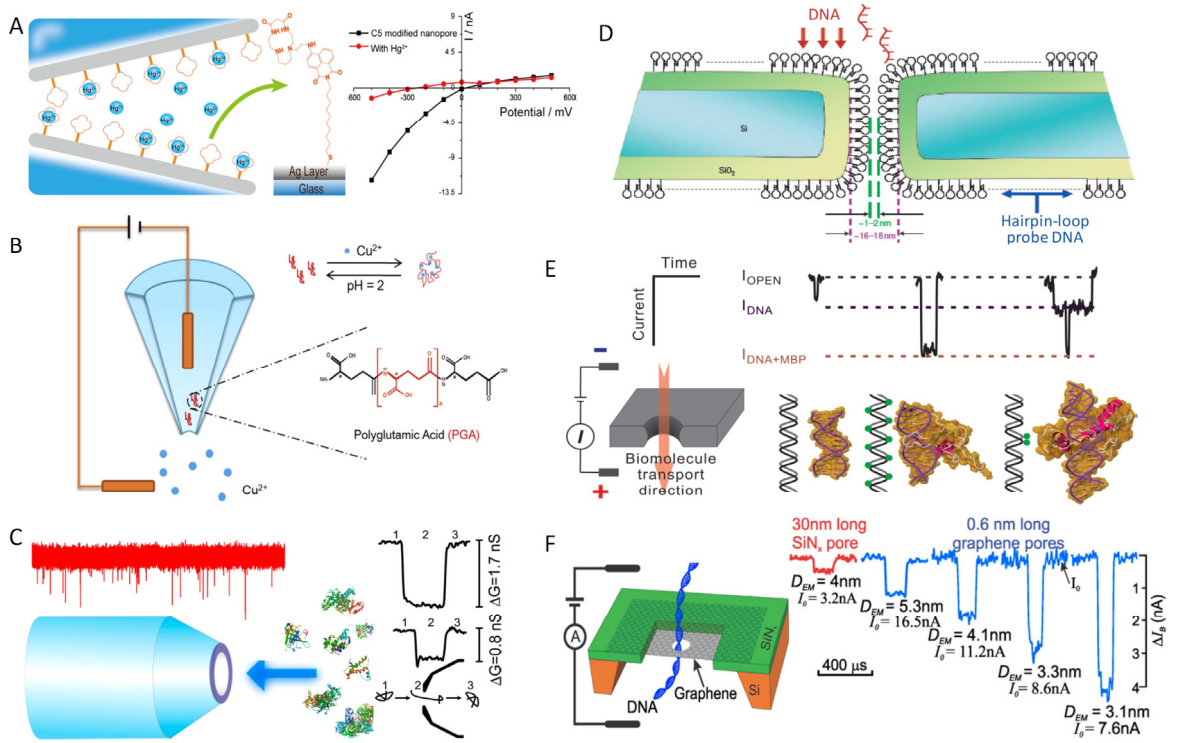

Figure 10 Inorganic nanopores for chemiresistive sensing. Glass nanopore used for (A) Hg^{2+} ions detection with C5 functionalized inner wall after coating with Ag layer, (Printed with permission from Reference [184]. ©2016 Springer.) (B) Cu^{2+} ion detection with a cupric selective chelating agent to increase the sensitivity (Printed with permission from Reference [185]. ©2015 Elsevier.) and (C) proteins translocation detection. (Printed with permission from Reference [186]. ©2013 American Chemical Society.) (D) Selective DNA detection with DNA probe functionalized in the inner wall. (Printed with permission from Reference [187]. ©2007 Nature Publishing Group.) (E) Ionic current characteristics for DNA methylation detection w/o MBPs. Enhanced current change can be observed at the translocation of the methylated DNA/MBPs complexes. (Printed with permission from Reference [188]. ©2015 American Chemical Society.) (F) DNA translocating through a graphene nanopore with different pore diameter: larger current change for smaller pore size. (Printed with permission from Reference [178, 189]. ©2013 The National Academy of Sciences of the USA.)

3.3.2 Biosensor

Inorganic solid-state nanopores are regarded as a promising substitution for protein nanopores in DNA sequencing in regard of mechanical and chemical stability. However, due to the limited current and time resolution, they did not show much improvement in sequencing [190]. Instead, nanopores has been adapted for single molecule investigation. The commonly used inorganic materials includes Si [187], SiO_2 [191], SiN [192, 193] membranes and glass/quartz capillaries [186, 194, 195]. Passing of charged molecules, e.g. proteins, DNA, through nanopores induces ionic conductivity reduction. The fast translocation of biomolecules raises time resolution problem for application in DNA sequencing. Slow down DNA translocation is a substantial challenge for solid state nanopores [196]. Several attempts have been proposed for this purpose: surface charge density modification [197], voltage control [192], salt concentration adjust [198], salt gradients creation [198], electrolyte selection, and transverse electric field control [199].

Glass nanopores have been applied for label-free sensing of proteins and DNA translocation events with resistive pulse technique [186, 194, 200-202]. Glass nanopores can be made by laser-assisted capillary-pulling [186, 201] or bench-top methods [203]. The pore size can be further shrank by electron irradiation down to 14 nm with improved signal-to-noise ratio [194]. Li et al. [186] demonstrated single protein molecule detection by ionic current (Fig. 10C). A list of proteins in solution: lysozyme, avidin, IgG, -lactoglobulin, ovalbumin, bovine serum albumin and -galactosidase are differentiated from their translocation direction, amplitude and event duration. The specific immobilization of lysozyme to aptamer induced surface charge change leads to a remarkable IV curve change with a detection limit as low as 5 pM [204].

While sensing with a large nanopores, DNA molecules, which have limited diameter of 2-5 nm, are difficult to detect or even no detectable. Iqbal et al. [187] functionalized a DNA probe to the nanopore walls and realized diameter reduction and selectively ssDNA detection (Fig. 10D). They observed longer translocation pulse and a significant translocation event reduction even with a single base mismatch between the probe and the target. In other cases, protein complexes are proposed to enhance electrical signal with application in healthcare and protein kinetics [205]. Shim et al. [188, 206] performed DNA methylation detection through a sub-10 nm nanopore. The methylated DNA selectively binds to methyl-binding proteins (MBPs). Enhanced current change demonstrates the translocation of the methylated DNA/MBPs complexes, as shown in Fig. 10E. This sensing technique proves to be very useful in studying the role of epigenetics in human disease.

Improve the DNA base resolution, atomic thin membranes, e.g. graphene [207], MoS_2 [208], boron nitride [209], drilled with nanopores are fabricated for DNA sequencing. The sensing scheme of these nanopores resembles SiN nanopores but have higher molecular resolution. Among these materials, graphene is the most studies material in recent years. It is a single layer of carbon atoms with a 2D hexagonal lattice arrangement, which represents an ultimate material for nanopore based sequencing. Other unique characteristics includes ions impenetrable, and electrical conducting. There are a few emerging sensing technologies based on graphene [11]. Garaj et al. [210] demonstrate that the effective insulating thickness of graphene membrane is within a nanometer, which makes graphene an ideal membrane for nanopore-based single molecule detectors, with high resolution and high throughput. They further reported DNA translocation events with this device and obtained the greatest sensitivity when the pore and molecule diameters are closely matched (Fig. 10F) [189]. Take advantage of the graphene's electrical conductive property, Traversi et al. [211] constructed a nanopore in graphene nanoribbon, which allows simultaneous translocation event detection by ionic current drop and graphene current change.

4. Convex/concave structures

Nanotubes, possess both convex and concave structures, are a material of great interest for wide applications. Carbon nanotubes (CNTs) in particular, have unique electrical, mechanical and chemical properties, are extremely sensitive to the chemical environment, and are regarded as the ultimate sensor. In this section, we focus on CNTs for application in gas sensing and biosensing.

4.1 Gas sensing

Gas sensing with CNTs takes advantage of both convex and concave surfaces. Charge transfer happens at the adsorption of gas molecules on CNTs. Single-walled CNT (SWCNT) consists entirely of surface with single carbon atom in thickness, allowing optimal interaction with molecules. Molecular gating to carbon NTs causes Fermi level shifting and therefore modulates the resistance. Collins et al. [212] revealed that CNT are extremely sensitive to gas exposure, and the electronic resistance can be reversibly modulated by exposure to air or oxygen. In the meanwhile, the first single-walled carbon nanotubes for gaseous molecule sensing such as NO_2, NH_3, is demonstrated by Kong et al. [213] CNT showed outstanding gas sensing characteristics with up to three orders of magnitude resistance change within several seconds of exposure to ppm level of NO_2, NH_3 flow at room temperature. The fast and sensitive response is attributed to the full exposure of the nanotube surface to sensing environment. Robinson et al. [214] specified that gas adsorption at defect sites of CNTs results in a large conductivity response as a result of the increased adsorbate binding energy and charge transfer at those defect sites. Therefore, by controlling defects introduction to CNTs, gas sensitivity can be improved.

For gas molecules including hydrogen and carbon monoxide, there is a lack of specific interaction with CNTs. Such interaction can be obtained through rational chemical and/or physical surface modification with noble metals, e.g. Pd, Pt, Rh and Au [215, 216], which can also improve selectivity for specific gas sensing. For example, Pd nanoparticle modified SWNT exhibits sensitive electrical sensing of hydrogen [216]. Park et al. [217] coated ultrathin carboxylated polypyrrole (CPPy) skin to CNT by vapor deposition polymerization for gas sensing at RT (Fig. 11A). The CPPy skin then provides stable attachment of Pd NPs on the surface with minimal skin thickness. The final nanohybrids (PCCNs) were constructed as FET sensor for hydrogen detection at a concentration limit of 1ppm. The dissolution of

hydrogen in Pd NPs resulted in a decrease in the Pd work function, which depleted the hole density in the p-type PCCN transducers. Therefore, increased resistance can be observed upon rising the hydrogen concentration. Another unique interface modification for gas sensing was realized by Staii et al. [218], who immobilized ssDNA through π-π stacking interaction with SWNTs. The base sequence of the ssDNA determines the gas response behavior. The fabricated devices achieved a variety of gas detection with fast response and recovery.

CNTs for VOCs detection present in the exhaled breath sample is another inspiring medical application. For such complex gas sample detection, cross-reactivity is an inevitable issue [219]. The key lies in the detection of disease through multi-sensor array, and identification of diseases through obtained data. Ionescu et al. [220] designed a cross-reactive array of SWCNTs, functionalized with polycyclic aromatic hydrocarbons for VOCs (hexanal, 5-methyl-undecane, and other compounds) detection. The sensors could discriminate between multiple sclerosis and healthy states from exhaled gas with over 80% accuracy. The same group later reported an artificially intelligent nanoarray based on SWNT network [221]. Clinical assessment proved that the nanoarray could classify 17 diseases from the exhaled breath via pattern analysis.

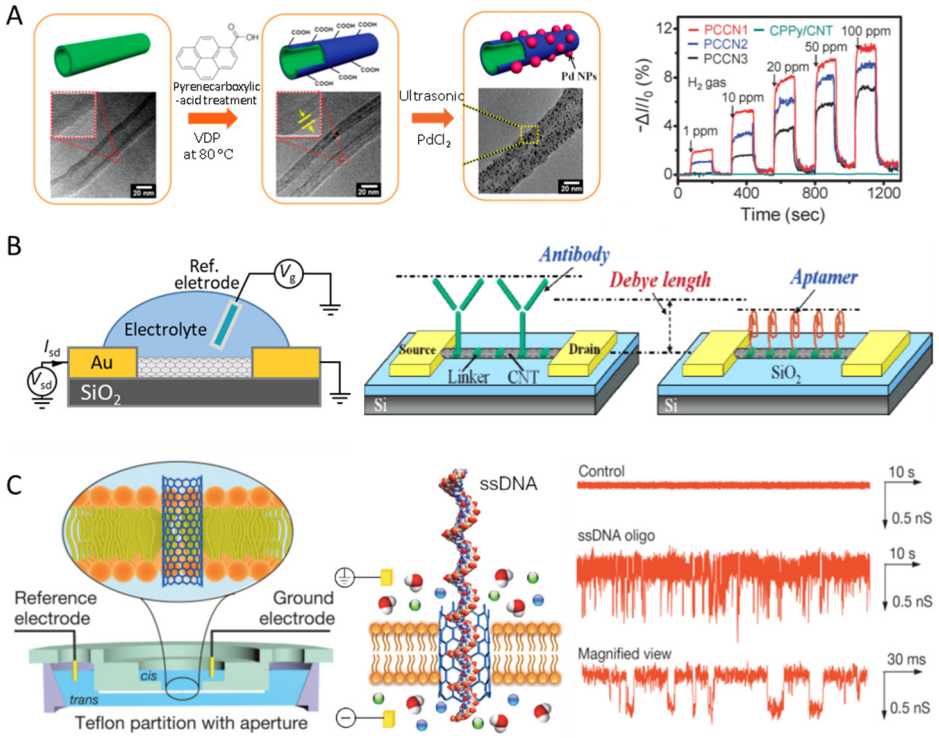

Figure 11 Carbon nanotubes (CNTs) as chemiresistive sensing. (A) Pt and carboxylated polypyrrole (CPPy) coated CNT for hydrogen gas sensing. (Printed with permission from Reference [217]. ©2013 Royal Society of Chemistry.) (B) Schematic of a single-walled CNT (SWNT) single FET device (left) and protein biosensor optimization: aptamer modified devices allow working in higher ionic concentration compared with antibody modified devices (right). (Printed with permission from Reference [222]. ©2007 American Chemical Society.) (C) CNT porins setup in a lipid bilayer (left), DNA translocation through CNT (middle) and conductance trances of ssDNA translocation signal (right). (Printed with permission from Reference [223]. ©2014 Nature Publishing Group.)

4.2 Biosensor

Construction of CNT for biosensing includes single CNT device (Fig. 11B) and CNT network device. The sensing mechanism of CNT biosensor is suggested to be the electrostatic gating and Schottky barrier

effects at the biomolecule adsorption on the surface [224]. The corresponding interface modifications are based either on molecules adsorption on CNT or on metal electrodes [225]. The applications include nucleic acid detection [225, 226], protein detection [227-229], and glucose sensing with enzyme-coated CNT [230-233]. To overcome the ion screening limitation, Maehashi et al. [222] modified CNT FET with aptamer for the detection of immunoglobulin E (IgE). The aptamer modified device showed better performance compared with antibody modified device owing to the smaller size (Fig. 11B).

Biomolecule immobilization to NTs can be achieved by noncovalent bonding [234] or covalent bonding [235]. The surface treatment of CNT differs from other materials as a result of the inactive carbon atom. The hydrophobic CNT surface allows noncovalent functionalization of surface with hydrocarbon chains or through hydrogen bond [236-238], e.g. polyethylene oxide and its derivatives [229]. The robust van der Waals interaction between hydrocarbon chain and CNT prevents molecule desorption. A wide range of aminated proteins and DNAs can be selectively immobilized covalently to the polymer layer using N-succinimidyl group and carbodiimide group [229, 236-238]. Martinez et al. synthesized poly(methylmethacrylata$_{0.6}$-co-poly(ethyleneglycol)methacrylate$_{0.15}$-co-N-succinimidyl-ethacrylate$_{0.25}$) that can noncovalently bond to CNTs [236]. Then the target layer, aminated ssDNA, was attached covalently to the polymer, which in the meantime inhibits the nonspecific adsorption of other DNA molecules. A versatile electrochemical immobilization method is developed by electropolymerizing 4-amino-benzoic acid onto the NT surface, which brings -COOH groups [237]. Then covalently couple aminated DNA. When measured at a frequency of 1 kHz, which ensures very low noise, DNA in realistic buffer solution can be detected at sub femtomolar concentration. For covalent bonding, defects need to be created such that biomolecules can be bonded [239, 240].

There are only a few examples of NTs sensor working as concave structures. Majority research on NT concave structure has been focused on the unique ionic transport due to the confined inner space [241, 242]. Kohli et al. [243] synthesized DNA-functionalized NT membranes to study the transport properties of DNA strands. The real resistive sensing application was realized by inserting sub-10 nm SWCNT in a lipid bilayer as substitution to α-HL [223, 244]. Geng et al. [223] inserted CNTs into lipid bilayers and live cell membranes for recording the stochastic transport of ions and ssDNA. Short CNTs with lengths of 5 – 15 nm was fixed to the bilayer as illustrated in Fig. 11C. The recorded conductance signal displays macromolecule-induced ionic current blockades characteristics.

5. Pros and cons of nanosensors with different structures

5.1 Gas sensor

The gas sensing with nanosensors is now approaching real-life application. Especially by taking advantage of the small size, devices can be made portable and inexpensive, and can be integrated into sensor arrays for complexed gas detection. Full exposure of atoms to gas for SWCNTs renders them higher sensitivity. One major concern of chemiresistive sensor of different structures for gas sensing is the stability. Compared with sensing in liquid, there is a lack of control over surface potential when working in air. The stability could be improved for example by encapsulating the active surface sites [90]. Another issue related with gas sensing is reusability of sensor by releasing the adsorbed gas molecules, e.g. how to properly integrate supplementary heating function to accelerate the gas diffusion [108]. Advanced techniques or materials need to be developed to tackle these problems.

5.2 Ionic sensor

Among the reviewed materials and structures, Si NWs are the most studied one for ionic sensing. Besides the high sensitivity nanostructure brings, one can benefit from the high spatial resolution of high density sensor array, e.g. for cellular local activity/environment monitoring [67, 245, 246]. However, selectivity, cross-reactivity, and drifting caused by ion diffusion remain challenging issues for their wide applications. Designing and preparing a stable interface material [74] and selective probes would benefit sensitive and selective detection.

The ionic sensing with nanopores is still in qualitative stage. The large amounts of ions present in solution limits the sensitivity for ionic sensing. Therefore, the sensing application is mainly limited in smart gating of NPs [129, 156]. There is very limited study on the ionic sensing with CNTs, most probably due to the inactive carbon surface to ions. Interface design on CNTs could be an effective way towards such application.

5.3 Biosensor

The DNA sensitivity for NW sensors has been shown to be down to fM level with high selectivity [61, 65, 237]. Besides the drifting issue caused by ions as mentioned in the previous section, another important consideration about such intrinsic charge-based sensing is the ionic screening effect. The commonly used low ionic strength solution extends screening length, lowers DNA hybridization rate, therefore, the pH and ion stability of low ionic solution prohibits its practical application. In the meanwhile, the liquid potential control with reference electrodes is more difficult. Especially when detecting in microchannels, streaming potential plays a significant role along the microchannels [247]. Further development of such nanosensors calls for either a stable and reliable detection environment or a differential setup [54, 248] to minimize those effect for application in biological fluidics.

NPs is a technique of high expectation for single molecule detection. The requirement of high spatial and time resolution involved in DNA sequencing raise a substantial question for solid-state NPs: how to minimize the noise for constructing a high signal-to-noise ratio device? Besides DNA sequencing, there are some reports on NP biosensor for biomolecule recognition and concentration detection. By taking advantage of NPs' curvature property [14], together with proper interface design, selective biomolecular detection could be a promising research direction for NPs.

While applied in medical diagnosis, reduction of false positive signal is critically important. One way out could be combining multiple sensors together, e.g. simultaneous potential detection with a NW and a NP [249]. By taking advantage of NWs' sensitivity and NTs concaved curvature, the atomic thin CNT material when designed in larger diameters, could be an ideal sensitive structure for biosensing.

6. Summaries and perspectives

In this review, we have presented the structural, material and interface designs, and the working mechanisms of chemiresistive nanosensor with special focus on convex and concave topography. Such extensive study offers new ideas and opportunities for potential application of aforementioned nanosensors. Materials of inorganic, organic to biologic have been applied to construct both convex and concave structured devices. The sensing principles differs for different materials, which can be

molecule adsorption induced material composition change, surface potential change or simply blocking effect. However, all these variables eventually can be characterized by resistance change. For both NWs and NPs, common interface design rules can be observed. Especially for selective ionic and biomolecule sensing, the recognition process is generally realized by the specific chemical or biological reaction between target and probe molecules.

The emerging new materials, interface design and device construction are pushing forward the development of chemiresistive sensors. The future work should focus on improving sensor stability, sensitivity, specificity, and the integration of such devices into portable intelligent equipments. We expect this review will promote scientific work on improving sensing performance of chemiresistive nanosensors with the aim to real-life applications.

Acknowledgements

This work was supported by the National Natural Science Foundation of China (grant numbers 61601387, 21673197, U1505243), the Natural Science Foundation of Fujian Province of China (grant number 2017J05107), Young Overseas High-level Talents Introduction Plan, the 111 Project (grant number B16029), the Open Funding of State Key Laboratory of Precision Measuring Technology and Instruments (grant number pilab1709), and the Fundamental Research Funds for the Central Universities of China (grant number 20720170050).

References

[1] Y. Cui, Q.Q. Wei, H.K. Park, C.M. Lieber, Science, 293 (2001) 1289-1292.

[2] A. Kolmakov, Y.X. Zhang, G.S. Cheng, M. Moskovits, Adv. Mater., 15 (2003) 997-1000.

[3] X. Hou, W. Guo, L. Jiang, Chem. Soc. Rev., 40 (2011) 2385-2401.

[4] N. Chartuprayoon, M.L. Zhang, W. Bosze, Y.H. Choa, N.V. Myung, Biosens. Bioelectron., 63 (2015) 432-443.

[5] S. Roy, Z.Q. Gao, Nano Today, 4 (2009) 318-334.

[6] J.E. Reiner, A. Balijepalli, J.W.F. Robertson, J. Campbell, J. Suehle, J.J. Kasianowicz, Chem. Rev., 112 (2012) 6431-6451.

[7] X. Hou, L. Jiang, ACS Nano, 3 (2009) 3339-3342.

[8] Y. Zhu, K. Zhan, X. Hou, ACS Nano, 12 (2018) 908-911.

[9] K.I. Chen, B.R. Li, Y.T. Chen, Nano Today, 6 (2011) 131-154.

[10] Z. Wang, S. Lee, K.I. Koo, K. Kim, IEEE T. Nanobiosci., 15 (2016) 186-199.

[11] S.J. Heerema, C. Dekker, Nat. Nanotechnol., 11 (2016) 127-136.

[12] E. Stern, J.F. Klemic, D.A. Routenberg, P.N. Wyrembak, D.B. Turner-Evans, A.D. Hamilton, et al., Nature, 445 (2007) 519-522.

[13] A. Mulchandani, N.V. Myung, Curr. Opin. Biotech., 22 (2011) 502-508.

[14] K. Shoorideh, C.O. Chui, Proc. Natl. Acad. Sci. USA., 111 (2014) 5111-5116.

[15] H. Shiigi, S. Tokonami, H. Yakabe, T. Nagaoka, J. Am. Chem. Soc., 127 (2005) 3280-3281.

[16] A. Kisner, M. Heggen, D. Mayer, U. Simon, A. Offenhausser, Y. Mourzina, Nanoscale, 6 (2014) 5146-5155.

[17] A. Bogozi, O. Lam, H. He, C. Li, N.J. Tao, L.A. Nagahara, et al., J. Am. Chem. Soc., 123 (2001) 4585-4590.

[18] F. Yang, S.C. Kung, M. Cheng, J.C. Hemminger, R.M. Penner, ACS Nano, 4 (2010) 5233-5244.

[19] F. Yang, D. Jung, R.M. Penner, Anal. Chem., 83 (2011) 9472-9477.

[20] P. Offermans, H.D. Tong, C.J.M. van Rijn, P. Merken, S.H. Brongersma, M. Crego-Calama, Appl. Phys. Lett., 94 (2009) 223110.

[21] F. Favier, E.C. Walter, M.P. Zach, T. Benter, R.M. Penner, Science, 293 (2001) 2227-2231.
[22] M.Z. Atashbar, D. Banerji, S. Singamaneni, P. Inter. Conf. Intell. Sensing Infor. Process., (2004) 185-189.
[23] F. Yang, D.K. Taggart, R.M. Penner, Nano Lett., 9 (2009) 2177-2182.
[24] C.G. Sonwane, J. Wilcox, Y.H. Ma, J. Phys. Chem. B, 110 (2006) 24549-24558.
[25] L.L. Tang, G. Yu, X.G. Li, F.F. Chang, C.J. Zhong, Chempluschem, 80 (2015) 722-730.
[26] R.C. Hughes, W.K. Schubert, J. Appl. Phys., 71 (1992) 542-544.
[27] Z. Liu, P.C. Searson, J. Phys. Chem. B, 110 (2006) 4318-4322.
[28] F. Yang, K.C. Donavan, S.C. Kung, R.M. Penner, Nano Lett., 12 (2012) 2924-2930.
[29] P. Shi, J.Y. Zhang, H.Y. Lin, P.W. Bohn, Small, 6 (2010) 2598-2603.
[30] H.W. Yoo, S.Y. Cho, H.J. Jeon, H.T. Jung, Anal. Chem., 87 (2015) 1480-1484.
[31] J. Wang, O. Rincon, R. Polsky, E. Dominguez, Electrochem. Commun., 5 (2003) 83-86.
[32] C. Russell, K. Welch, J. Jarvius, Y.X. Cai, R. Brucas, F. Nikolajeff, et al., ACS Nano, 8 (2014) 1147-1153.
[33] Y. Weizmann, D.M. Chenoweth, T.M. Swager, J. Am. Chem. Soc., 133 (2011) 3238-3241.
[34] E. Braun, Y. Eichen, U. Sivan, G. Ben-Yoseph, Nature, 391 (1998) 775-778.
[35] H.A. Becerril, R.M. Stoltenberg, C.F. Monson, A.T. Woolley, J. Mater. Chem., 14 (2004) 611-616.
[36] J. Richter, R. Seidel, R. Kirsch, M. Mertig, W. Pompe, J. Plaschke, et al., Adv. Mater., 12 (2000) 507-510.
[37] Z.X. Deng, C.D. Mao, Nano Lett., 3 (2003) 1545-1548.
[38] M. Mertig, L.C. Ciacchi, R. Seidel, W. Pompe, A. De Vita, Nano Lett., 2 (2002) 841-844.
[39] Y. Cui, C.M. Lieber, Science, 291 (2001) 851-853..
[40] L. Bousse, N.F. de Rooij, P. Bergveld, IEEE T. Electron. Dev., 30 (1983) 1263-1270.
[41] A. van den Berg, P. Bergveld, D.N. Reinhoudt, E.J.R. Sudholter, Sens. Actuators, 8 (1985) 129-148.
[42] R.E.G. van Hal, J.C.T. Eijkel, P. Bergveld, Sens. Actuators B, 24 (1995) 201-205.
[43] D.E. Yates, S. Levine, T.W. Healy, J. Chem. Soc. Faraday Trans. 1, 70 (1974) 1807-1818.
[44] J.C.T. Eijkel, A. van den Berg, Chem. Soc. Rev., 39 (2010) 957-973.
[45] O. Knopfmacher, A. Tarasov, W.Y. Fu, M. Wipf, B. Niesen, M. Calame, et al., Nano Lett., 10 (2010) 2268-2274.
[46] A. Tarasov, M. Wipf, R.L. Stoop, K. Bedner, W.Y. Fu, V.A. Guzenko, et al., ACS Nano, 6 (2012) 9291-9298.
[47] S. Chen, J.G. Bomer, E.T. Carlen, A. van den Berg, Nano Lett., 11 (2011) 2334-2341.
[48] X.X. Duan, Y. Li, N.K. Rajan, D.A. Routenberg, Y. Modis, M.A. Reed, Nat. Nanotechnol., 7 (2012) 401-407.
[49] G.F. Zheng, X.P.A. Gao, C.M. Lieber, Nano Lett., 10 (2010) 3179-3183.
[50] S. Chen, J.W. van Nieuwkasteele, A. van den Berg, J.C.T. Eijkel, Anal. Chem., 88 (2016) 7890-7893.
[51] S. Zafar, C. D'Emic, A. Afzali, B. Fletcher, Y. Zhu, T. Ning, Nanotechnology, 22 (2011) 405501.
[52] Y.L. Bunimovich, Y.S. Shin, W.S. Yeo, M. Amori, G. Kwong, J.R. Heath, J. Am. Chem. Soc., 128 (2006) 16323-16331.
[53] L.B. Luo, J.S. Jie, W.F. Zhang, Z.B. He, J.X. Wang, G.D. Yuan, et al., Appl. Phys. Lett., 94 (2009) 193101.
[54] M. Wipf, R.L. Stoop, A. Tarasov, K. Bedner, W.Y. Fu, I.A. Wright, et al., ACS Nano, 7 (2013) 5978-5983.
[55] G.F. Zheng, F. Patolsky, Y. Cui, W.U. Wang, C.M. Lieber, Nat. Biotechnol., 23 (2005) 1294-1301.
[56] N. Shehada, G. Bronstrup, K. Funka, S. Christiansen, M. Leja, H. Haick, Nano Lett., 15 (2015) 1288-1295.
[57] X.L. Luo, J.J. Davis, Chem. Soc. Rev., 42 (2013) 5944-5962.
[58] J.H. Chua, R.E. Chee, A. Agarwal, S.M. Wong, G.J. Zhang, Anal. Chem., 81 (2009) 6266-6271.
[59] E. Stern, A. Vacic, N.K. Rajan, J.M. Criscione, J. Park, B.R. Ilic, et al., Nat. Nanotechnol., 5 (2010) 138-142.
[60] A.R. Gao, N. Lu, P.F. Dai, C.H. Fan, Y.L. Wang, T. Li, Nanoscale, 6 (2014) 13036-13042.
[61] J. Hahm, C.M. Lieber, Nano Lett., 4 (2004) 51-54.
[62] Y.L. Bunimovich, Y.S. Shin, W.S. Yeo, M. Amori, G. Kwong, J.R. Heath, J. Am. Chem. Soc., 128 (2006) 16323-16331.

[63] Z.Q. Gao, A. Agarwal, A.D. Trigg, N. Singh, C. Fang, C.H. Tung, et al., Anal. Chem., 79 (2007) 3291-3297.
[64] Z.C. Fang, S.O. Kelley, Anal. Chem., 81 (2009) 612-617.
[65] M.N.M. Nuzaihan, U. Hashim, M.K.M. Arshad, S.R. Kasjoo, S.F.A. Rahman, A.R. Ruslinda, M.F.M. Fathil, R. Adzhri, M.M. Shahimin, Biosens. Bioelectron., 83 (2016) 106-114.
[66] F. Patolsky, G.F. Zheng, O. Hayden, M. Lakadamyali, X.W. Zhuang, C.M. Lieber, Proc. Natl. Acad. Sci. USA, 101 (2004) 14017-14022.
[67] Q. Qing, S.K. Pal, B.Z. Tian, X.J. Duan, B.P. Timko, T. Cohen-Karni, et al., Proc. Natl. Acad. Sci. USA, 107 (2010) 1882-1887.
[68] E. Stern, E.R. Steenblock, M.A. Reed, T.M. Fahmy, Nano Lett., 8 (2008) 3310-3314.
[69] T. Cohen-Karni, B.P. Timko, L.E. Weiss, C.M. Lieber, Proc. Natl. Acad. Sci. USA, 106 (2009) 7309-7313.
[70] B.P. Timko, T. Cohen-Karni, G.H. Yu, Q. Qing, B.Z. Tian, C.M. Lieber, Nano Lett., 9 (2009) 914-918.
[71] T. Cohen-Karni, Q. Qing, Q. Li, Y. Fang, C.M. Lieber, Nano Lett., 10 (2010) 1098-1102.
[72] F. Patolsky, G.F. Zheng, C.M. Lieber, Nat. Protoc., 1 (2006) 1711-1724.
[73] A.R. Gao, N. Lu, Y.L. Wang, T. Li, Sci. Rep.-UK, 6 (2016) 22554.
[74] B.R. Dorvel, B. Reddy, J. Go, C.D. Guevara, E. Salm, M.A. Alam, R. Bashir, ACS Nano, 6 (2012) 6150-6164.
[75] X. Duan, L.Y. Mu, S.D. Sawtelle, N.K. Rajan, Z.Y. Han, Y.Y. Wang, et al., Adv. Funct. Mater., 25 (2015) 2279-2286.
[76] M.N. Masood, S. Chen, E.T. Carlen, A. van den Berg, ACS Appl. Mater. Inter., 2 (2010) 3422-3428.
[77] T. Kong, R.G. Su, B.B. Zhang, Q. Zhang, G.S. Cheng, Biosens. Bioelectron., 34 (2012) 267-272.
[78] E. Stern, R. Wagner, F.J. Sigworth, R. Breaker, T.M. Fahmy, M.A. Reed, Nano Lett., 7 (2007) 3405-3409.
[79] P.R. Nair, M.A. Alam, Nano Lett., 8 (2008) 1281-1285.
[80] G.J. Zhang, G. Zhang, J.H. Chua, R.E. Chee, E.H. Wong, A. Agarwal, et al., Nano Lett., 8 (2008) 1066-1070.
[81] E. Stern, R. Wagner, F.J. Sigworth, R. Breaker, T.M. Fahmy, M.A. Reed, Nano Lett., 7 (2007) 3405-3409.
[82] M. Ferrari, Nat. Rev. Cancer, 5 (2005) 161-171.
[83] D.P. Tran, B. Wolfrum, R. Stockmann, J.H. Pai, M. Pourhassan-Moghaddam, A. Offenhausser, et al., Anal. Chem., 87 (2015) 1662-1668.
[84] N. Gao, W. Zhou, X.C. Jiang, G.S. Hong, T.M. Fu, C.M. Lieber, Nano Lett., 15 (2015) 2143-2148.
[85] R. Elnathan, M. Kwiat, A. Pevzner, Y. Engel, L. Burstein, A. Khatchtourints, et al., Nano Lett., 12 (2012) 5245-5254.
[86] V. Krivitsky, M. Zverzhinetsky, F. Patolsky, Nano Lett., 16 (2016) 6272-6281.
[87] C.J. Chu, C.S. Yeh, C.K. Liao, L.C. Tsai, C.M. Huang, H.Y. Lin, et al., Nano Lett., 13 (2013) 2564-2569.
[88] J. Li, G. He, H. Ueno, C.C. Jia, H. Noji, C.M. Qi, X.F. Guo, Nanoscale, 8 (2016) 16172-16176.
[89] R. Ermanok, O. Assad, K. Zigelboim, B. Wang, H. Haick, ACS Appl. Mater. Inter., 5 (2013) 11172-11183.
[90] J.M. Halpern, B. Wang, H. Haick, ACS Appl. Mater. Inter., 7 (2015) 11315-11321.
[91] B. Wang, J.C. Cancilla, J.S. Torrecilla, H. Haick, Nano Lett., 14 (2014) 933-938.
[92] A. Miranda, F. de Santiago, L.A. Perez, M. Cruz-Irisson, Sensor. Actuat. B-Chem., 242 (2017) 1246-1250.
[93] O.H. Elibol, D. Morisette, D. Akin, J.P. Denton, R. Bashir, Appl. Phys. Lett., 83 (2003) 4613-4615.
[94] M.C. McAlpine, H. Ahmad, D.W. Wang, J.R. Heath, Nat. Mater., 6 (2007) 379-384.
[95] Y. Paska, T. Stelzner, S. Christiansen, H. Haick, ACS Nano, 5 (2011) 5620-5626.
[96] N. Shehada, J.C. Cancilla, J.S. Torrecilla, E.S. Pariente, G. Bronstrup, S. Christiansen, et al., ACS Nano, 10 (2016) 7047-7057.
[97] Y. Paska, H. Haick, ACS Appl. Mater. Interfaces, 4 (2012) 2604-2617.
[98] Y. Engel, R. Elnathan, A. Pevzner, G. Davidi, E. Flaxer, F. Patolsky, Angew. Chem. Int. Ed., 49 (2010) 6830-6835.
[99] Y.M. Chu, C.C. Lin, H.C. Chang, C.M. Li, C.X. Guo, Biosens. Bioelectron., 26 (2011) 2334-2340.
[100] E. Comini, C. Baratto, G. Faglia, M. Ferroni, A. Vomiero, G. Sberveglieri, Prog. Mater. Sci., 54 (2009) 1-67.

[101] M. Bogner, A. Fuchs, K. Scharnagl, R. Winter, T. Doll, I. Eisele, Appl. Phys. Lett., 73 (1998) 2524-2526.
[102] D.H. Dawson, D.E. Williams, J. Mater. Chem., 6 (1996) 409-414.
[103] T.V. Dang, N.D. Hoa, N.V. Duy, N.V. Hieu, ACS Appl. Mater. Interfaces, 8 (2016) 4828-4837.
[104] S. Roso, F. Guell, P.R. Martinez-Alanis, A. Urakawa, E. Llobet, Sens. Actuators B, 230 (2016) 109-114.
[105] Y.L. Wang, X.C. Jiang, Y.N. Xia, J. Am. Chem. Soc., 125 (2003) 16176-16177.
[106] J.D. Prades, A. Cirera, J.R. Morante, J.M. Pruneda, P. Ordejon, Sens. Actuators B, 126 (2007) 62-67.
[107] Q. Wan, T.H. Wang, Chem. Commun., (2005) 3841-3843.
[108] J.D. Prades, R. Jimenez-Diaz, F. Hernandez-Ramirez, S. Barth, A. Cirera, A. Romano-Rodriguez, et al., Appl. Phys. Lett., 93 (2008) 123110
[109] D.H. Lien, J.R.D. Retamal, J.J. Ke, C.F. Kang, J.H. He, Nanoscale, 7 (2015) 19874-19884.
[110] A. Kolmakov, D.O. Klenov, Y. Lilach, S. Stemmer, M. Moskovits, Nano Lett., 5 (2005) 667-673.
[111] X.M. Zou, J.L. Wang, X.Q. Liu, C.L. Wang, Y. Jiang, Y. Wang, et al., Nano Lett., 13 (2013) 3287-3292.
[112] A.Z. Sadek, W. Wlodarski, K. Kalantar-Zadeh, C. Baker, R.B. Kaner, Sens. Actuators A, 139 (2007) 53-57.
[113] J. Janata, M. Josowicz, Nat. Mater., 2 (2003) 19-24.
[114] C.M. Hangarter, M. Bangar, A. Mulchandani, N.V. Myung, J. Mater. Chem., 20 (2010) 3131-3140.
[115] W.S. Huang, B.D. Humphrey, A.G. Macdiarmid, J. Chem. Soc. Faraday Trans. 1, 82 (1986) 2385-2400.
[116] C.J. Liu, Z. Noda, K. Sasaki, K. Hayashi, Int. J. Hydrogen Energ., 37 (2012) 13529-13535.
[117] Y.J. Wang, K.K. Coti, W. Jun, M.M. Alam, J.J. Shyue, W.X. Lu, et al., Nanotechnology, 18 (2007) 424021.
[118] H.Q. Liu, J. Kameoka, D.A. Czaplewski, H.G. Craighead, Nano Lett., 4 (2004) 671-675.
[119] N. Tang, Y. Jiang, H. Qu, X. Duan, Nanotechnology, (2017) 485301.
[120] E. Song, J.W. Choi, Sens. Actuators B, 215 (2015) 99-106.
[121] D.T. McQuade, A.E. Pullen, T.M. Swager, Chem. Rev., 100 (2000) 2537-2574.
[122] J.A. Arter, D.K. Taggart, T.M. McIntire, R.M. Penner, G.A. Weiss, Nano Lett., 10 (2010) 4858-4862.
[123] K. Ramanathan, M.A. Bangar, M. Yun, W. Chen, N.V. Myung, A. Mulchandani, J. Am. Chem. Soc., 127 (2005) 496-497.
[124] M.A. Bangar, D.J. Shirale, H.J. Purohit, W. Chen, N.V. Myung, A. Mulchandani, Electroanal., 23 (2011) 371-379.
[125] H. Yoon, S. Ko, J. Jang, J. Phys. Chem. B, 112 (2008) 9992-9997.
[126] E.S. Forzani, H.Q. Zhang, L.A. Nagahara, I. Amlani, R. Tsui, N.J. Tao, Nano Lett., 4 (2004) 1785-1788.
[127] M.A. Bangar, D.J. Shirale, W. Chen, N.V. Myung, A. Mulchandani, Anal. Chem., 81 (2009) 2168-2175.
[128] J.A. Arter, J.E. Diaz, K.C. Donavan, T. Yuan, R.M. Penner, G.A. Weiss, Anal. Chem., 84 (2012) 2776-2783.
[129] Z. Zhang, L.P. Wen, L. Jiang, Chem. Soc. Rev., 47 (2018) 322-356.
[130] E. Gouaux, R. Mackinnon, Science, 310 (2005) 1461.
[131] X. Kang, S. Cheley, R.F. And, H. Bayley, J. Am. Chem. Soc., 129 (2007) 4701-4705.
[132] M. Wanunu, T. Dadosh, V. Ray, J. Jin, L. Mcreynolds, M. Drndić, Nat. Nanotechnol., 5 (2010) 807.
[133] T.Z. Butler, M. Pavlenok, I.M. Derrington, M. Niederweis, J.H. Gundlach, Proc. Natl. Acad. Sci. USA, 105 (2008) 20647.
[134] G. Maglia, M.R. Restrepo, E. Mikhailova, H. Bayley, Proc. Natl. Acad. Sci. USA, 105 (2008) 19720-19725.
[135] J.J. Kasianowicz, E. Brandin, D. Branton, D.W. Deamer, Proc. Natl. Acad. Sci. USA, 93 (1996) 13770-13773.
[136] J. Clarke, H.C. Wu, L. Jayasinghe, A. Patel, S. Reid, H. Bayley, Nat. Nanotechnol., 4 (2009) 265-270.
[137] D. Rotem, L. Jayasinghe, M. Salichou, H. Bayley, J. Am. Chem. Soc., 134 (2012) 2781.
[138] O. Braha, L.Q. Gu, L. Zhou, X. Lu, S. Cheley, H. Bayley, Nat. Biotechnol., 18 (2000) 1005-1007.
[139] O. Braha, B. Walker, S. Cheley, J.J. Kasianowicz, L. Song, J.E. Gouaux, H. Bayley, Chem. Biol., 4 (1997) 497.
[140] A.F. Hammerstein, S.H. Shin, H. Bayley, Angew. Chem. Int. Ed. Engl., 49 (2010) 5085-5090.

[141] S. Wen, T. Zeng, L. Liu, K. Zhao, Y.L. Zhao, X.J. Liu, H.C. Wu, J. Am. Chem. Soc., 133 (2011) 18312-18317.
[142] G.H. Wang, L. Wang, Y.J. Han, S. Zhou, X.Y. Guan, Biosens. Bioelectron., 53 (2014) 453-458.
[143] Y. Astier, A. Orit Braha, H. Bayley, J. Am. Chem. Soc., 128 (2006) 1705.
[144] E. Epstein, Int. Rev. Cytol., 34 (1973) 123-168.
[145] J.C. Skou, Physiol. Rev., 45 (1965) 596.
[146] Q. Wang, H. Wang, X. Fan, J. Zhai, Sci. Adv. Mater., 7 (2015) 2147-2167.
[147] X. Hou, L. Jiang, ACS Nano, 3 (2009) 3339.
[148] W. Guo, H. Xia, F. Xia, X. Hou, L. Cao, L. Wang, et al., Chemphyschem A, 11 (2010) 859.
[149] X. Hou, H. Dong, D. Zhu, L. Jiang, Small, 6 (2010) 361-365.
[150] L. Wen, X. Hou, Y. Tian, F.Q. Nie, Y. Song, J. Zhai, L. Jiang, Adv. Mater., 22 (2010) 1021-1024.
[151] X. Hou, Y. Liu, H. Dong, F. Yang, L. Li, L. Jiang, Adv. Mater., 22 (2010) 2440.
[152] C. Han, X. Hou, H. Zhang, W. Guo, H. Li, L. Jiang, J. Am. Chem. Soc., 133 (2011) 7644-7647.
[153] Y. Tian, X. Hou, L. Jiang, J. Electroanal. Chem., 656 (2011) 231-236.
[154] Y. Tian, L. Wen, X. Hou, G. Hou, L. Jiang, Chemphyschem, 13 (2012) 2455.
[155] X. Hou, F. Yang, L. Li, Y. Song, L. Jiang, D. Zhu, J. Am. Chem. Soc., 132 (2010) 11736-11742.
[156] H. Xu, Adv. Mater., 28 (2016) 7049-7064.
[157] R.L. Fleischer, P.B. Price, R.M. Walker, Nuclear Tracks in Solids: Principles and Applications, University of California Press, Berkeley, 1975.
[158] S. Howorka, Z. Siwy, Chem. Soc. Rev., 38 (2009) 2360-2384.
[159] C.C. Harrell, Z.S. Siwy, C.R. Martin, Small, 2 (2006) 194-198.
[160] E.A. Heins, Z.S. Siwy, L.A. Baker, C.R. Martin, Nano Lett., 5 (2005) 1824.
[161] Z.S. Siwy, Adv. Funct. Mater., 16 (2010) 735-746.
[162] Z. Siwy, A. Fuliński, Phys. Rev. Lett., 89 (2002) 198103.
[163] D. Dobrev, J. Vetter, R. Neumann, N. Angert, J. Vac. Sci. Technol. B, 19 (2001) 1385-1387.
[164] S. Lee, Y. Zhang, H.S. White, C.C. Harrell, C.R. Martin, Anal. Chem., 76 (2004) 6108-6115.
[165] H.C. Zhang, Y. Tian, L. Jiang, Nano Today, 11 (2016) 61-81.
[166] F. Xia, W. Guo, Y.D. Mao, X. Hou, J.M. Xue, H.W. Xia, et al., J. Am. Chem. Soc., 130 (2008) 8345-8350.
[167] X. Hou, W. Guo, F. Xia, F.Q. Nie, H. Dong, Y. Tian, et al., J. Am. Chem. Soc., 131 (2009) 7800-7805.
[168] G. Perez-Mitta, A.G. Albesa, W. Knoll, C. Trautmann, M.E. Toimil-Molares, O. Azzaroni, Nanoscale, 7 (2015) 15594-15598.
[169] G. Perez-Mitta, A.G. Albesa, C. Trautmann, M.E. Toimil-Molares, O. Azzaroni, Chem. Sci., 8 (2017) 890-913.
[170] Z. Zhang, P. Li, X.Y. Kong, G.H. Xie, Y.C. Qian, Z.Q. Wang, et al., J. Am. Chem. Soc., 140 (2018) 1083-1090.
[171] A. Mara, Z. Siwy, C. Trautmann, A.J. Wan, F. Kamme, Nano Lett., 4 (2004) 497-501.
[172] K. Healy, B. Schiedt, A.P. Morrison, Nanomedicine-UK, 2 (2007) 875.
[173] K. Kececi, L.T. Sexton, F. Buyukserin, C.R. Martin, Nanomedicine-UK, 3 (2008) 787.
[174] Z. Siwy, L. Trofin, P. Kohli, L.A. Baker, C. Trautmann, C.R. Martin, J. Am. Chem. Soc., 127 (2005) 5000-5001.
[175] P. Waduge, R. He, P. Bandarkar, H. Yamazaki, B. Cressiot, Q. Zhao, et al., ACS Nano, 11 (2017) 5706-5716.
[176] Y. He, D. Gillespie, D. Boda, I. Vlassiouk, R.S. Eisenberg, Z.S. Siwy, J. Am. Chem. Soc., 131 (2009) 5194-5202.
[177] M. Ali, B. Yameen, R. Neumann, W. Ensinger, W. Knoll, O. Azzaroni, J. Am. Chem. Soc., 130 (2008) 16351-16357.
[178] M. Ali, R. Neumann, W. Ensinger, ACS Nano, 4 (2010) 7267-7274.
[179] C.C. Harrell, Y. Choi, L.P. Horne, L.A. Baker, Z.S. Siwy, C.R. Martin, Langmuir, 22 (2006) 10837.
[180] N.N. Liu, Y.N. Jiang, Y.H. Zhou, F. Xia, W. Guo, L. Jiang, Angew. Chem. Int. Ed., 52 (2013) 2007-2011.
[181] W. Guo, F. Hong, N.N. Liu, J.Y. Huang, B.Y. Wang, R.X. Duan, et al., Adv. Mater., 27 (2015) 2090-2095.

[182] Y.L. Xu, X. Sui, S. Guan, J. Zhai, L.C. Gao, Adv. Mater., 27 (2015) 1851-1855.
[183] X.M. Shang, G.H. Xie, X.Y. Kong, Z. Zhang, Y.Q. Zhang, W. Tian, et al., Adv. Mater., 29 (2017) 1603884 .
[184] R. Gao, Y.L. Ying, B.Y. Yan, P. Iqbal, J.A. Preece, X.Y. Wu, Microchim. Acta, 183 (2016) 491-495.
[185] L.Z. Chen, H.L. He, X.L. Xu, Y.D. Jin, Anal. Chim. Acta, 889 (2015) 98-105.
[186] W. Li, N.A.W. Bell, S. Hernandez-Ainsa, V.V. Thacker, A.M. Thackray, R. Bujdoso, et al., ACS Nano, 7 (2013) 4129-4134.
[187] S.M. Iqbal, D. Akin, R. Bashir, Nat. Nanotechnol., 2 (2007) 243-248.
[188] J. Shim, Y. Kim, G.I. Humphreys, A.M. Nardulli, F. Kosari, G. Vasmatzis, et al., ACS Nano, 9 (2015) 290-300.
[189] S. Garaj, S. Liu, J.A. Golovchenko, D. Branton, Proc. Natl. Acad. Sci. USA, 110 (2013) 12192-12196.
[190] F. Liang, P.M. Zhang, Sci. Bull., 60 (2015) 296-303.
[191] A.J. Storm, J.H. Chen, X.S. Ling, H.W. Zandbergen, C. Dekker, Nat. Mater., 2 (2003) 537.
[192] M. Firnkes, D. Pedone, J. Knezevic, M. Doblinger, U. Rant, Nano Lett., 10 (2010) 2162-2167.
[193] I. Yanagi, T. Ishida, K. Fujisaki, K. Takeda, Sci Rep-UK, 5 (2015).
[194] L.J. Steinbock, R.D. Bulushev, S. Krishnan, C. Raillon, A. Radenovic, ACS Nano, 7 (2013) 11255-11262.
[195] J.P. Guerrette, B. Zhang, J. Am. Chem. Soc., 132 (2010) 17088-17091.
[196] D. Branton, D.W. Deamer, A. Marziali, H. Bayley, S.A. Benner, T. Butler, et al., Nat. Biotechnol., 26 (2008) 1146-1153.
[197] A.J. Storm, C. Storm, J.H. Chen, H. Zandbergen, J.F. Joanny, C. Dekker, Nano Lett., 5 (2005) 1193-1197.
[198] R.M.M. Smeets, U.F. Keyser, D. Krapf, M.Y. Wu, N.H. Dekker, C. Dekker, Nano Lett., 6 (2006) 89-95.
[199] J. Lagerqvist, M. Zwolak, M. Di Ventra, Nano Lett., 6 (2006) 779-782.
[200] J. Bafna, G. Soni, Biophys. J., 110 (2016) 503A.
[201] X.Q. Gong, A.V. Patil, A.P. Ivanov, Q.Y. Kong, T. Gibb, F. Dogan, et al., Anal. Chem., 86 (2014) 835-841.
[202] L.J. Steinbock, S. Krishnan, R.D. Bulushev, S. Borgeaud, M. Blokesch, L. Feletti, et al., Nanoscale, 6 (2014) 14380-14387.
[203] B. Zhang, J. Galusha, P.G. Shiozawa, G.L. Wang, A.J. Bergren, R.M. Jones,et al., Anal. Chem., 79 (2007) 4778-4787.
[204] S.L. Cai, S.H. Cao, Y.B. Zheng, S. Zhao, J.L. Yang, Y.Q. Li, Biosens. Bioelectron., 71 (2015) 37-43.
[205] K.J. Freedman, A.R. Bastian, I. Chaiken, M.J. Kim, Small, 9 (2013) 750-759.
[206] J. Shim, G.I. Humphreys, B.M. Venkatesan, J.M. Munz, X.Q. Zou, C. Sathe,et al., Sci. Rep.-UK, 3 (2013).
[207] Z.S. Siwy, M. Davenport, Nat. Nanotechnol., 2 (2010) 697-698.
[208] K. Liu, J.D. Feng, A. Kis, A. Radenovic, ACS Nano, 8 (2014) 2504-2511.
[209] S. Liu, B. Lu, Q. Zhao, J. Li, T. Gao, Y.B. Chen, et al., Adv. Mater., 25 (2013) 4549-4554.
[210] S. Garaj, W. Hubbard, A. Reina, J. Kong, D. Branton, J.A. Golovchenko, Nature, 467 (2010) 190-193.
[211] F. Traversi, C. Raillon, S.M. Benameur, K. Liu, S. Khlybov, M. Tosun, et al., Nat. Nanotechnol., 8 (2013) 939-945.
[212] P.G. Collins, K. Bradley, M. Ishigami, A. Zettl, Science, 287 (2000) 1801-1804.
[213] J. Kong, N.R. Franklin, C.W. Zhou, M.G. Chapline, S. Peng, K.J. Cho, et al., Science, 287 (2000) 622-625.
[214] J.A. Robinson, E.S. Snow, S.C. Badescu, T.L. Reinecke, F.K. Perkins, Nano Lett., 6 (2006) 1747-1751.
[215] A. Star, V. Joshi, S. Skarupo, D. Thomas, J.C.P. Gabriel, J. Phys. Chem. B, 110 (2006) 21014-21020.
[216] J. Kong, M.G. Chapline, H.J. Dai, Adv. Mater., 13 (2001) 1384-1386.
[217] S.J. Park, O.S. Kwon, J. Jang, Chem. Commun., 49 (2013) 4673-4675.
[218] C. Staii, A.T. Johnson, Nano Lett., 5 (2005) 1774-1778.
[219] D.R. Kauffman, A. Star, Angew. Chem. Int. Ed., 47 (2008) 6550-6570.
[220] R. Ionescu, Y. Broza, H. Shaltieli, D. Sadeh, Y. Zilberman, X.L. Feng, et al., ACS Chem. Neurosci., 2 (2011) 687-

693.
[221] M.K. Nakhleh, H. Amal, R. Jeries, Y.Y. Broza, M. Aboud, A. Gharra, et al., ACS Nano, 11 (2017) 112-125.
[222] K. Maehashi, T. Katsura, K. Kerman, Y. Takamura, K. Matsumoto, E. Tamiya, Anal. Chem., 79 (2007) 782-787.
[223] J. Geng, K. Kim, J.F. Zhang, A. Escalada, R. Tunuguntla, L.R. Comolli, et al., Nature, 514 (2014) 612-615.
[224] I. Heller, A.M. Janssens, J. Mannik, E.D. Minot, S.G. Lemay, C. Dekker, Nano Lett., 8 (2008) 591-595.
[225] X.W. Tang, S. Bansaruntip, N. Nakayama, E. Yenilmez, Y.L. Chang, Q. Wang, Nano Lett., 6 (2006) 1632-1636.
[226] A. Star, E. Tu, J. Niemann, J.C.P. Gabriel, C.S. Joiner, C. Valcke, Proc. Natl. Acad. Sci. USA., 103 (2006) 921-926.
[227] A.M. Munzer, W.J. Seo, G.J. Morgan, Z.P. Michael, Y. Zhao, K. Melzer, et al., J. Phys. Chem. C, 118 (2014) 17193-17199.
[228] H.L. Qi, C. Ling, R. Huang, X.Y. Qiu, S.G. Li, Q. Gao, C.X. Zhang, Electrochim. Acta, 63 (2012) 76-82.
[229] R.J. Chen, S. Bangsaruntip, K.A. Drouvalakis, N.W.S. Kam, M. Shim, Y.M. Li, et al., Proc. Natl. Acad. Sci. USA, 100 (2003) 4984-4989.
[230] K.W. Kim, B.C. Kim, H.J. Lee, J. Kim, M.K. Oh, Electroanal., 23 (2011) 980-986.
[231] S. Bi, H. Zhou, S.S. Zhang, Biosens. Bioelectron., 24 (2009) 2961-2966.
[232] Y.D. Wang, P.P. Joshi, K.L. Hobbs, M.B. Johnson, D.W. Schmidtke, Langmuir, 22 (2006) 9776-9783.
[233] K. Besteman, J.O. Lee, F.G.M. Wiertz, H.A. Heering, C. Dekker, Nano Lett., 3 (2003) 727-730.
[234] H. Vedala, Y.A. Chen, S. Cecioni, A. Imberty, S. Vidal, A. Star, Nano Lett., 11 (2011) 170-175.
[235] Y.H. Yun, Z.Y. Dong, V. Shanov, W.R. Heineman, H.B. Halsall, A. Bhattacharya, et al., Nano Today, 2 (2007) 30-37.
[236] M.T. Martinez, Y.C. Tseng, N. Ormategui, I. Loinaz, R. Eritja, J. Bokor, Nano Lett., 9 (2009) 530-536.
[237] T. Kurkina, A. Vlandas, A. Ahmad, K. Kern, K. Balasubramanian, Angew. Chem. Int. Ed., 50 (2011) 3710-3714.
[238] A. Star, J.C.P. Gabriel, K. Bradley, G. Gruner, Nano Lett., 3 (2003) 459-463.
[239] S. Banerjee, T. Hemraj-Benny, S.S. Wong, Adv. Mater., 17 (2005) 17-29.
[240] Y.B. Wang, Z. Iqbal, S.V. Malhotra, Chem. Phys. Lett., 402 (2005) 96-101.
[241] B.J. Hinds, N. Chopra, T. Rantell, R. Andrews, V. Gavalas, L.G. Bachas, Science, 303 (2004) 62-65.
[242] J.K. Holt, H.G. Park, Y.M. Wang, M. Stadermann, A.B. Artyukhin, C.P. Grigoropoulos, et al., Science, 312 (2006) 1034-1037.
[243] P. Kohli, C.C. Harrell, Z.H. Cao, R. Gasparac, W.H. Tan, C.R. Martin, Science, 305 (2004) 984-986.
[244] L. Liu, C. Yang, K. Zhao, J.Y. Li, H.C. Wu, Nat. Commun., 4 (2013) 2989
[245] F. Patolsky, B.P. Timko, G.H. Yu, Y. Fang, A.B. Greytak, G.F. Zheng, et al., Science, 313 (2006) 1100-1104.
[246] B.Z. Tian, T. Cohen-Karni, Q. Qing, X.J. Duan, P. Xie, C.M. Lieber, Science, 329 (2010) 830-834.
[247] S.Y. Chen, Y.B. Xie, A. De, A. van den Berg, E.T. Carlen, Appl. Phys. Lett., 103 (2013).
[248] A. Tarasov, M. Wipf, K. Bedner, J. Kurz, W. Fu, V.A. Guzenko, et al., Langmuir, 28 (2012) 9899-9905.
[249] P. Xie, Q.H. Xiong, Y. Fang, Q. Qing, C.M. Lieber, Nat. Nanotechnol., 7 (2012) 119-125.

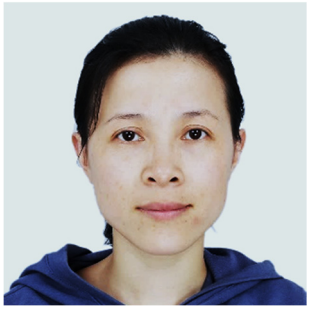

Dr. Songyue Chen received B.S. degree in 2004 from Zhejiang University, China. She completed Ph.D. in 2011 at University of Twente, the Netherlands. She did her postdoctoral research in Mesa+ Institute for Nanotechnology in University of Twente (2013-2015). Now she is an associated professor at Xiamen University. Her current research interests include micro/nanosensors and their applications in bio/chemical sensing.

Yongliang Tang is currently a master student in Songyue Chen's Group at Xiamen University, China. His main research direction is fabrication and characterization of nanopore-based sensors.

Dr. Kan Zhan received PhD degree at the University of Tokyo (2017), Japan under the direction of Prof. Hirotaka Ejima and Naoko Yoshie. Now he does the postdoctoral research in Prof. Xu Hou's Group at Xiamen University. His Current research interests include bio-inspired materials, liquid-based membranes, and smart polymeric membranes.

Dr Daoheng Sun is currently a professor at Xiamen University, and associate Dean of School of Aerospace Engineering. He received his B.S. degree (1987), M.S. degree (1990), and Ph.D. degree (1997) from Northeast University, China. He worked as visiting scholar in UC Berkley (2004-2005). His scientific interests are focused on MEMS/NEMS, micro/nano sensors and actuators, micro/nano 3D printing, etc.

Dr. Xu Hou received his B.Sc. degree (2006) from Sichuan University. He completed his Ph.D. (2011) at the National Center for Nanoscience and Technology, China, under the direction of Prof. Lei Jiang. He did postdoctoral research in Prof. Joanna Aizenberg's group at Harvard University (2012–2015). Now he is a full professor in both College of Chemistry & Chemical Engineering and College of Physical Science & Technology at Xiamen University, China. His research group mainly focuses on bio-inspired and smart multi-scale pore/channel systems, polymer materials, membrane science & technology, microfluidics, interfacial science, physical chemistry, electrochemistry, nano/micro fabrication for energy-saving and biomedical applications.